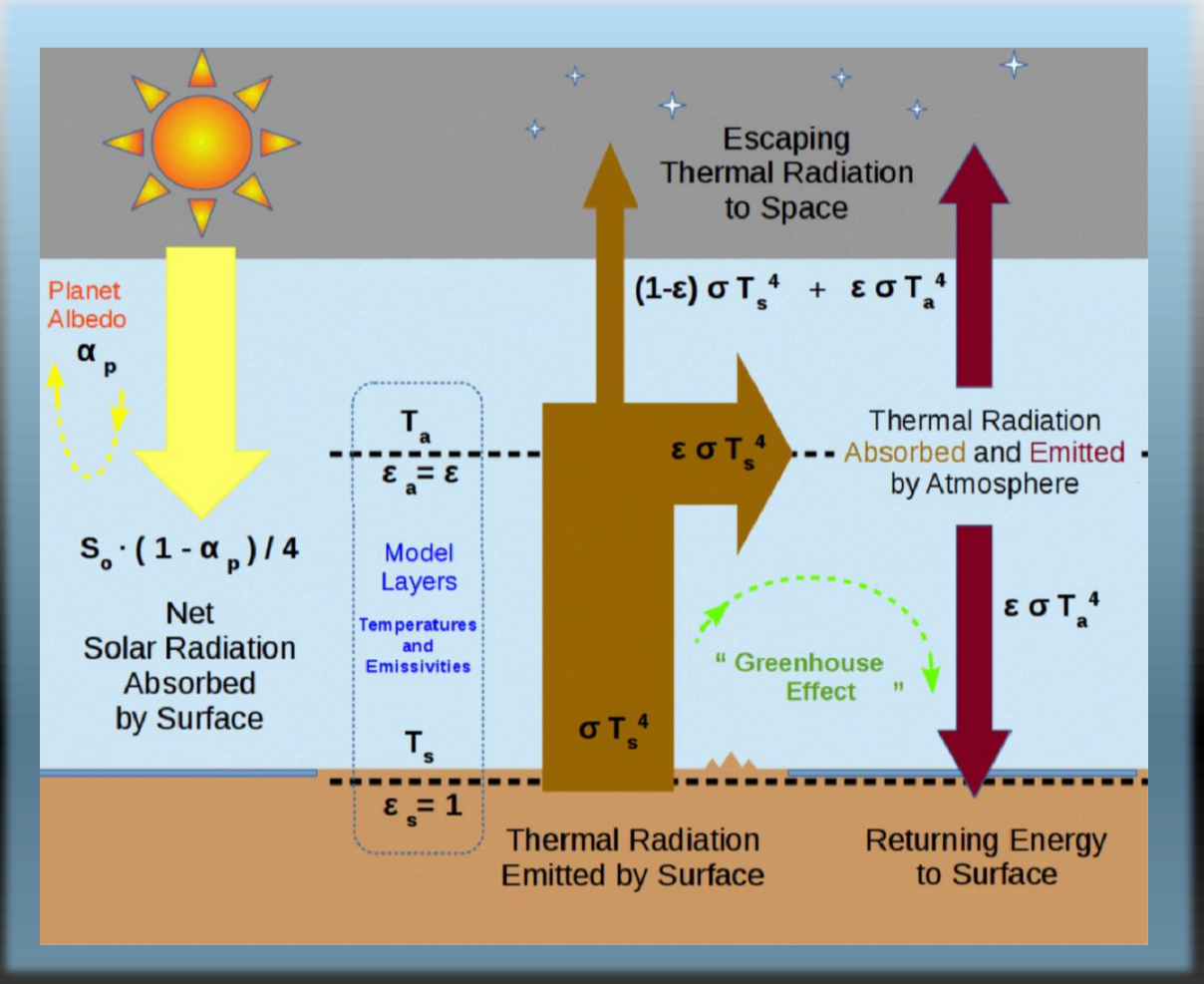

INVESTIGATION OF THE GREENHOUSE ATMOSPHERIC CARBON DIOXIDE EFFECTS ON GLOBAL WARMING

This report discusses simple models to investigate the claims of anthropogenic (man- caused) climate changes (viz., global warming). Specifically, the models investigate the magnitude of the atmospheric CO_2 contribution to global warming.
The author greatly acknowledges J. Roger Hill, Ph.D. for his many helpful suggestions and references.

J. Regnald Curry, Ph.D.

Table of Contents

List of Figures

INVESTIGATION OF THE GREENHOUSE CO_2 EFFECT ON GLOBAL WARMING

J. Regnald Curry[1]

1. INTRODUCTION

Predictions of anthropogenic global warming and climate change are investigated using several climate change models. The first two are simple models from a Penn State University online course[2]. In addition, a more sophisticated model based on a finite difference solution to the First Law of Thermodynamics is used to further examine potential global warming. The investigation examines the contribution of the greenhouse gas, CO_2, to climate change. This is important because current global warming alarmists claim the dominant culprit is human emissions of CO_2. Specifically, they claim the use of fossil fuels is by far the worst contributor to global warming; therefore, fossil fuels must be replaced with "green energy" sources immediately.

2. SIMPLE ENERGY BALANCE MODEL (EBM)

The Energy Balance Model (EBM) is the simplest model to explain the average surface temperature of the Earth. This model assumes the incident energy flux from the sun is balanced by the energy flux radiated away from the Earth. Even though the model is simple, it is adjusted through the emissivity

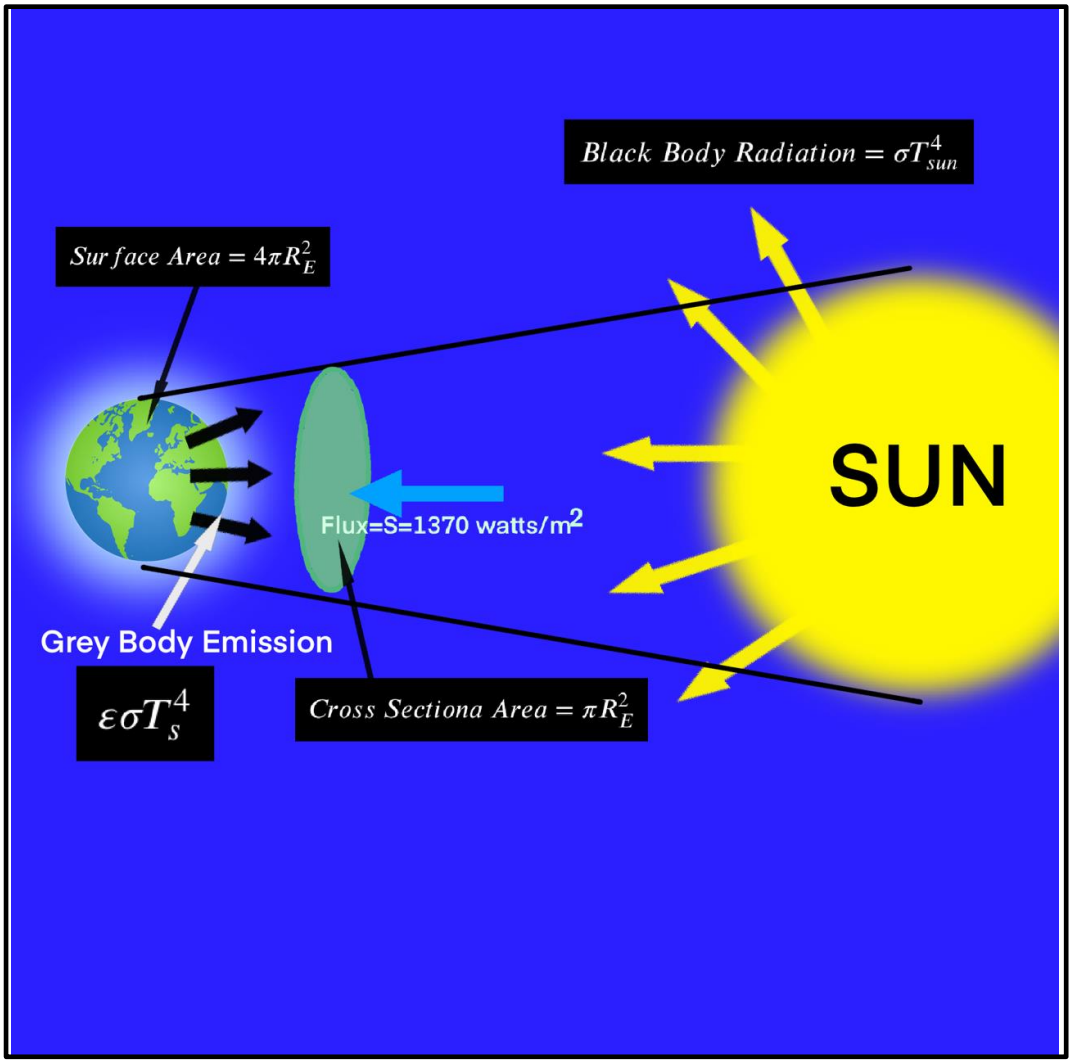

Figure 1. Simple Energy Balance Model; Overview

of the Earth to approximate the downward radiation from the greenhouse gas (CO_2) effect in the atmosphere. A pictorial overview of the energy balance is shown in Figure 1.

The temperature of the sun is given by: $T_{sun} = 5770°K$

The Stefan-Boltzmann Constant is given by: $\sigma = 5.6704 \cdot 10^{-8} watts/(m^2 °K^4)$

The Black Body Flux from the Sun is given by: $F_{sun} = \sigma {T_{sun}}^4 = 6.285 \cdot 10^7\ watts/m^2$

The Radius of the Sun is given by: $R_{sun} = 7.0 \cdot 10^8 meters$

The Solar Luminosity (constant power output of sun) is given by:

$$L_{sun} = 4\pi R_{sun}^2 \cdot F_{sun} = 3.87 \cdot 10^{26} watts$$

Average Distance from Sun to Earth is given by: $R_{SE} = 1.5 \cdot 10^{11} meters$

Therefore, the Average Sun's energy flux at the Earth is given by:

$$F_{earth} = \frac{L_{sun}}{4\pi R_{SE}^2} = 1.36877 \cdot 10^3 \frac{watts}{m^2}$$

This is approximately equal to the accepted value for the Solar Constant = $S = 1370 watts/m^2$

The radius of the Earth is $R_E = 6371 km$

So, the incident energy at the Earth is given by: $E_{incident} = S\pi R_E^2 = 1.747 \cdot 10^{17} watts$

And, the energy emitted back into space by the Earth is given by the Earths gray body radiation:

$$E_{emitted} = 4\pi R_E^2 (\epsilon \sigma T_s^4)$$

The value of ϵ is 1.0 for a perfect black body radiator and 0.0 for a perfect absorber of radiation. If $0 \le \varepsilon \le 1.0$ we have a gray body radiator, or an imperfect black body.

The net energy incident on the Earth is: $E_{net\ incident} = S\pi R_E^2 (1 - \alpha) = 1.188 \cdot 10^{17} watts$

Where α = the average reflectivity of Earth's surface looking down from space, i.e., the planetary albedo, which accounts for reflection by clouds and the atmosphere as well as the reflective surface of the Earth, including ice.
α≈0.32

Referring to Figure 1, the important constants and formulas to calculate the EBM results are presented in the blue text box.

"T_s represents the average skin temperature of an Earth covered by 70% ocean. The ocean is treated as a mixed layer of average 70m depth; this ignores the impacts of heat exchange with the deep ocean but is not a bad first approximation. We approximate the thermodynamic effect of the mixed layer ocean in terms of an *effective heat capacity* of the Earth's "land-ocean" surface, where C=2.08x10^{8}Joules/(°K ·m^2). The condition of energy balance can then be described in terms of thermodynamics, which states that any change in the internal energy per unit area per unit time ($\Delta F \approx C \cdot dT_s/dt$) must balance the rate of net heating, which is the difference between the incoming shortwave and outgoing longwave radiation." [2] Mathematically, that gives:

$$C\frac{dT_s}{dt} = \frac{S(1-\alpha)}{4} - (\epsilon \sigma T_s^4) \qquad (1)$$

Therefore, at thermal equilibrium, we have energy balance, where:

$$C\frac{dT_s}{dt} = 0$$

Therefore,

$$\epsilon \sigma T_s^4 = \frac{S(1-\alpha)}{4}$$

Solving for T_s gives: $T_s = \sqrt[4]{\frac{S(1-\alpha)}{4\epsilon\sigma}} \approx 253°K \approx -20°C \approx -4°F$ if,ϵ = 1.0, a perfect black body!

This results in a FROZEN PLANET! This happens because greenhouse gases have not been included in the model. These atmospheric gasses result in some of the emitted radiation being re-radiated back toward the Earth to warm the planet. Without greenhouse gases, Earth would not be a very pleasant planet for humans.

The variation in Earth's temperature from 1883 to 2023 is 0.4%. Therefore, the following linearization of the T_s^4 can be used to approximate T_s^4 fairly accurately. Linearization is a common mathematical tool to evaluate functions that do not vary significantly over the domain of interest. The inset figure shows

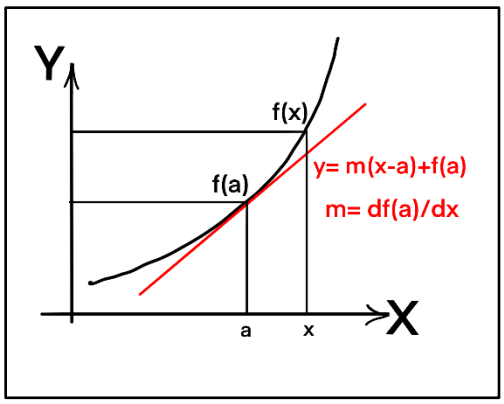

the details of the process. Again, the function f(x) is assumed to have only small variations over the range of X from a to x. Applying this to the above gives the following.

$$\frac{S(1-\alpha)}{4} = A + B(T_s - T_o) \qquad (2)$$

where, $A = \epsilon\sigma T_o^4$ and $B = 4\epsilon\sigma T_o^3$. Solving for T_s gives.

$$T_s = \frac{\left[\frac{S \cdot (1-\alpha)}{4} - A\right]}{B} + T_o$$

This can also be derived from the binomial expansion where $\Delta T_s / T_o << 1$. We set $T_o = 14\ ^oC$ to match the stated average global temperature from 1950 to 1980, as reported by NASA[5]. The emissivity (ϵ) is set to 0.6062 to approximate a gray body Earth and thus account for the atmosphere. The result is a more reasonable value for the Earth's surface temperature.

$$T_S = 286.906K$$

We will use these values for the remainder of the EBM analyses to obtain a time-dependent T_s versus the documented CO_2 greenhouse gas concentration in the atmosphere.

3. GREENHOUSE GAS (CO_2) CONCENTRATION DATA

The CO_2 concentration in the Earth's atmosphere for the past 800,000 years is provided in Figure 2. This curve is exemplary of those causing "climate alarm" over the past several decades [3]. It is the time scale that makes the increase between 1880 and 2023 appear so dramatic.

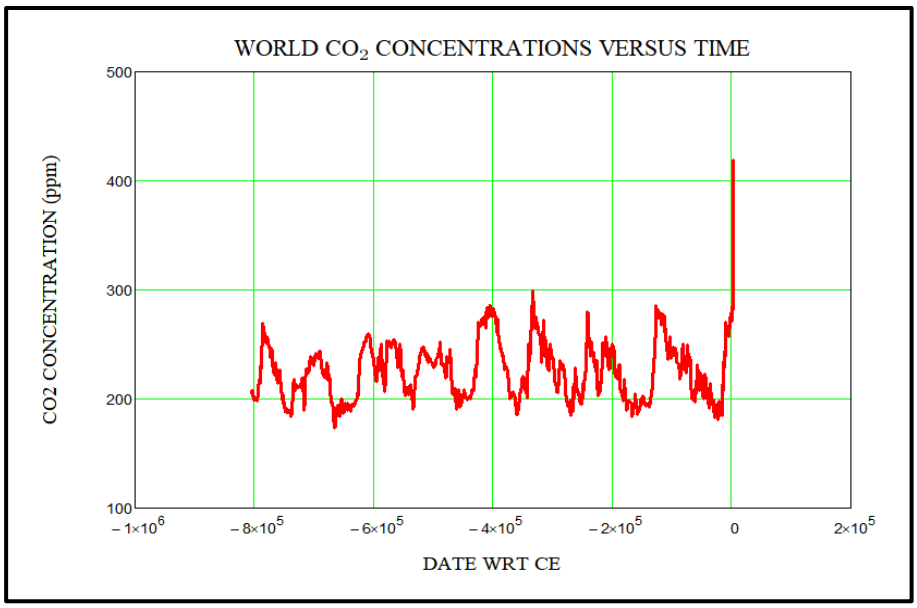

Figure 2. World Atmospheric CO_2 Concentration (ppm) in 2023 and 800,000 Years Prior

From here on, we will concentrate on the more recent past (1880–2023) to see the effect of the industrial revolution on the CO_2 concentration in the Earth's atmosphere. Then, using the above model and the reported CO_2 radiative forcing function, we will determine the magnitude of CO_2 radiative forcing on the actual surface temperature of the Earth.

If we plot the above data only for the time period between 1880 and 2023, we get the results shown in **Figure 3**. This curve is much less alarming because the time scale is reduced. Nevertheless, the preponderance of climate scientists uses this curve to predict catastrophic climate events in the future. They focus on the variation of temperature instead of the absolute temperature, which we will

use herein; however, as later noted, anomaly data normalized to different time ranges causes confusion and misinterpretation of results.

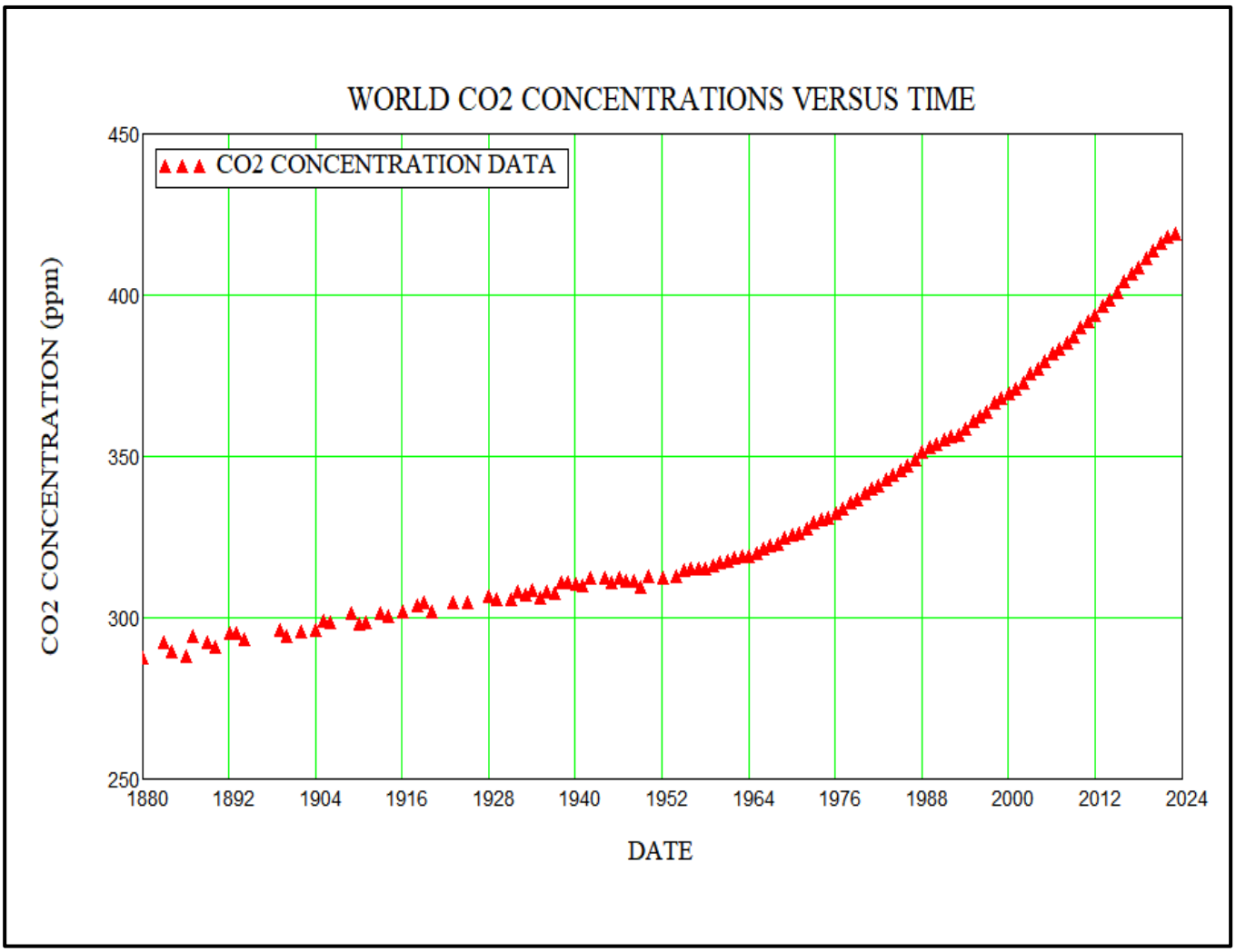

Figure 3. CO_2 Atmospheric Concentration 1880–2023

Before we examine the change in surface temperature due to CO_2 radiative forcing, we fit the CO_2 curve (Figure 3) and then extrapolate to future dates based on standard fitting and extrapolation techniques.

Two fits to the CO_2 atmospheric concentration data are summarized in **Figure 4**. The entire data set in Figure 3 is fit with a log-log interpolation. Then a third-order polynomial regression is used to fit the data between 1980 and 2023. The regression is extended to 2053 to enable model predictions for the next thirty years. The resulting CO_2 concentration curve of Figure 4 is used in the models to account for the greenhouse gas effects on climate change.

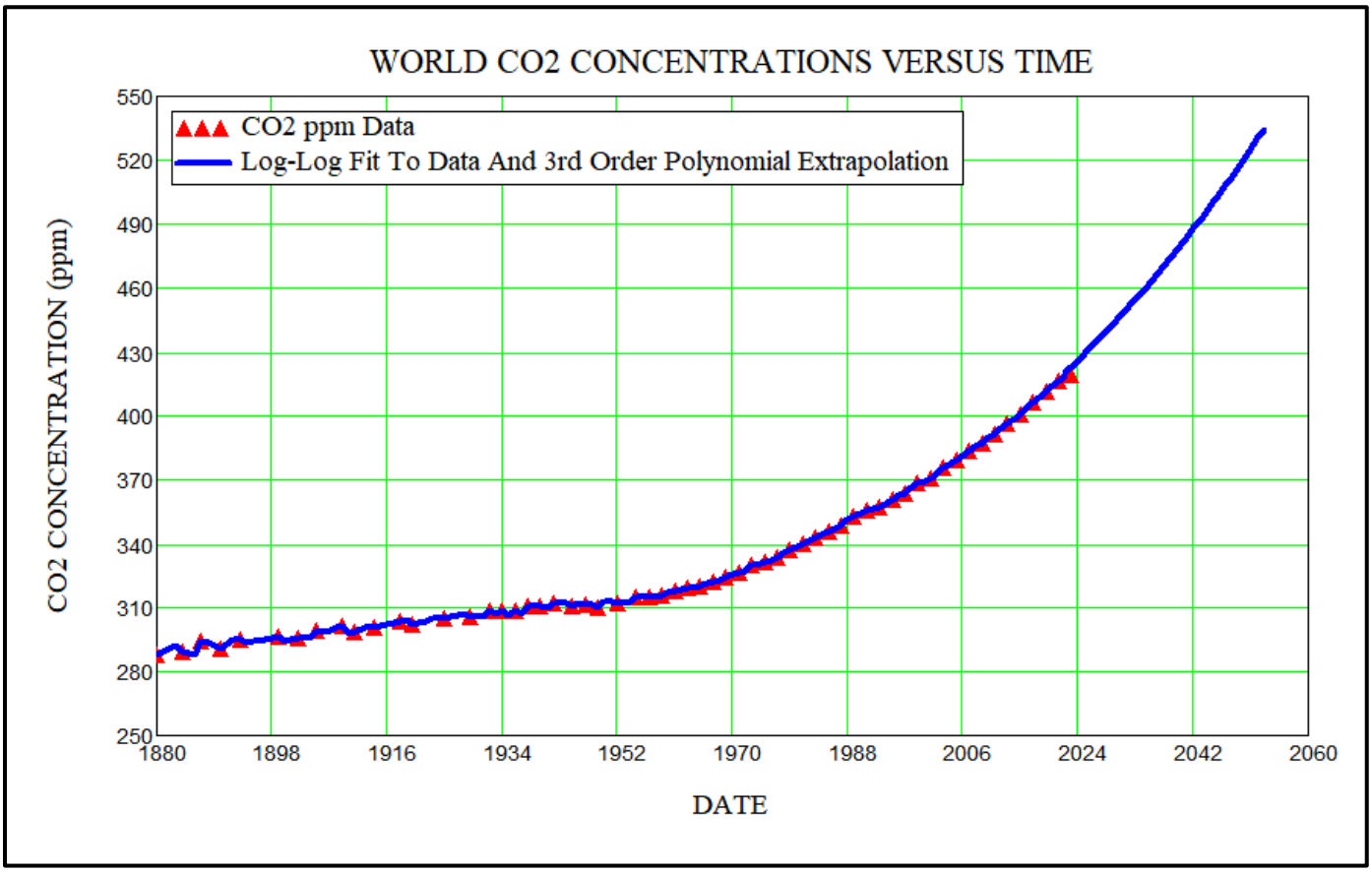

Figure 4. Fit and Projection of CO_2 Data 1880–2053

4. EBM SURFACE TEMPERATURE FOR CO_2 GREENHOUSE EFFECT

Recall the previous formula for the Earth's surface temperature. Reviewing the definitions given in Section 2, the following defines the incident energy flux as:

$$\Phi_{in} = \frac{S \cdot (1-\alpha)}{4} \tag{3}$$

The surface temperature is then given by the following.

$$T_s = \frac{\left[\frac{S \cdot (1-\alpha)}{4} - A\right]}{B} + T_o$$

$$T_s = \frac{[\Phi_{in} - A]}{B} + T_o$$

Now, we will define Φ_{in} as representing the total incoming radiative energy flux at the surface, which includes incoming shortwave radiation plus any potential changes in the downward longwave radiation toward the surface. When the greenhouse effect is present, the temperature at the surface, T_s, will be higher due to the additional downward longwave radiation emitted by the atmosphere toward the Earth's surface.

Consider the response of T_s to an incremental change in Φ_{in}. Since the sun's flux, A and T_0 are constants, we have the following change in T_s due to a change in the incident energy flux from the downward radiation emitted by the atmosphere.

$$\Delta T_s = \frac{\Delta \Phi_{in}}{B}$$

The change in downward longwave radiation forcing associated with a change in CO_2 concentration from a reference value, $[CO_2]_0$, to some new value, $[CO_2]$, is approximated by the following relationship from a paper by Myhre et al. [4]

$$\Delta F_{CO_2} = 5.35 ln\left(\frac{[CO_2]}{[CO_2]_0}\right)\frac{W}{m^2} \quad (4)$$

Where $[CO_2]_0 = 287.771(ppm)$, which is the CO_2 concentration at 1880 from the actual data in Figure 3. The CO_2 concentration at any given time is $[CO_2]$; The value of $[CO_2]$ is the fit to the CO_2 data as given in Figure 4.

Therefore, the CO_2 greenhouse gas effect on the surface temperature is given by the following.

$$\Delta T_{CO_2} = \frac{\Delta F_{CO_2}}{B} \quad \text{and} \quad (5)$$

$$T_s = T_0 + \Delta T_{CO_2}$$

Where T_0 = 14°C (57.2°F), the reference surface temperature defined in Section 2. Applying this to the CO_2 concentrations of Figure 4, our model for the Earth's surface temperature from 1883 to 2053 is given in **Figure 5**. These are absolute temperatures rather than variations from some "ideal temperature." The normalization value of T_0 = 14 °C is shown in the figure for illustrative purposes. It will be used in later sections of the report.

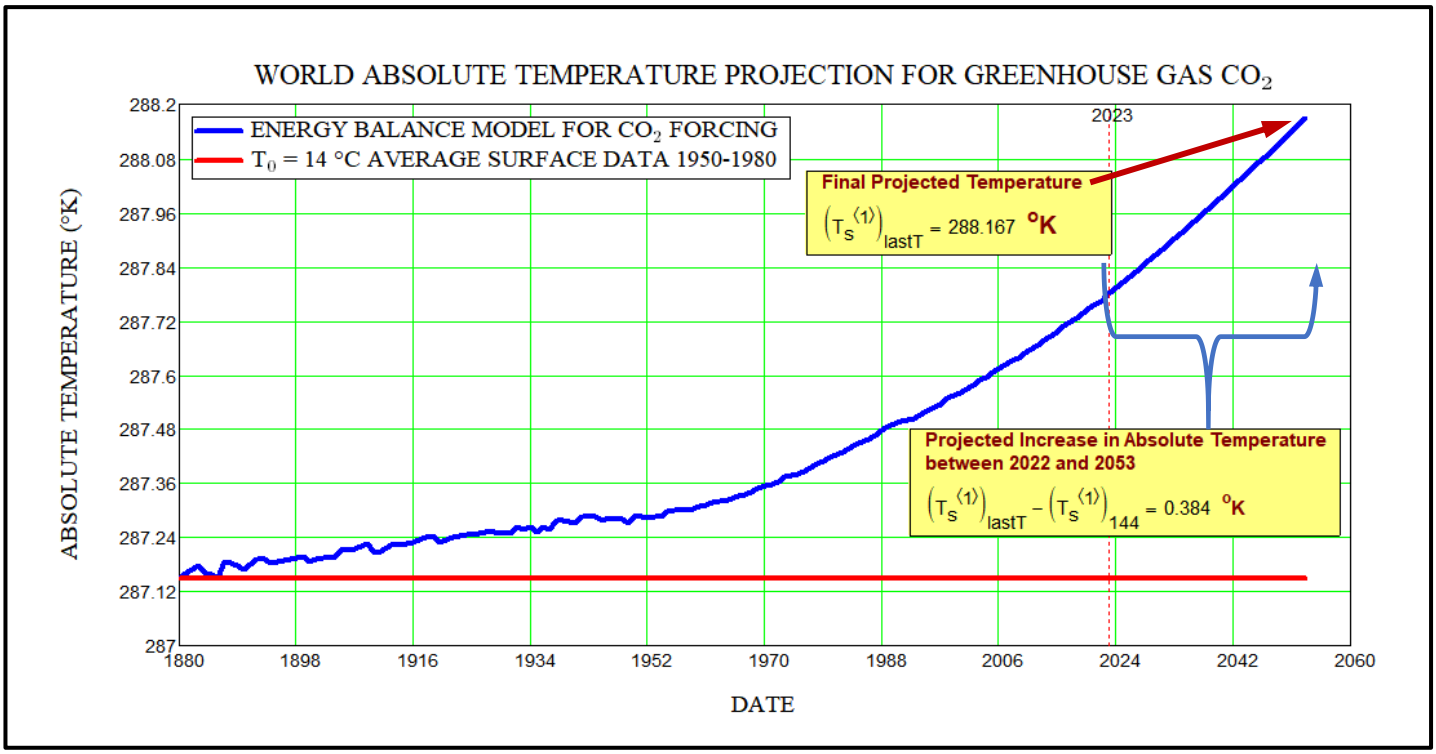

Figure 5. Earth Surface Temperatures in Kelvin for CO_2 Greenhouse Gas Effect

Most climate change publications are in terms of a temperature anomaly from some “ideal” reference temperature. Because the NASA surface temperature data is normalized to T_0 = 14 ^oC, the Energy Balance Model is normalized to that same temperature between 1950 and 1980 to compare with the surface temperature data. The results are shown in **Figure 6**.

Almost all references to climate change are in terms of a surface temperature anomaly normalized to some ideal temperature. As noted, Figure 6 compares the CO_2 forcing model anomaly with the NASA surface temperature data. The fit is rather poor at later dates and well below the data. However, other data is available, namely satellite infrared measurements of the temperature of the lower troposphere[6]. This data is significant because it provides lower troposphere (figure right) temperatures where all the weather occurs. This comparison is shown in **Figure 7**.

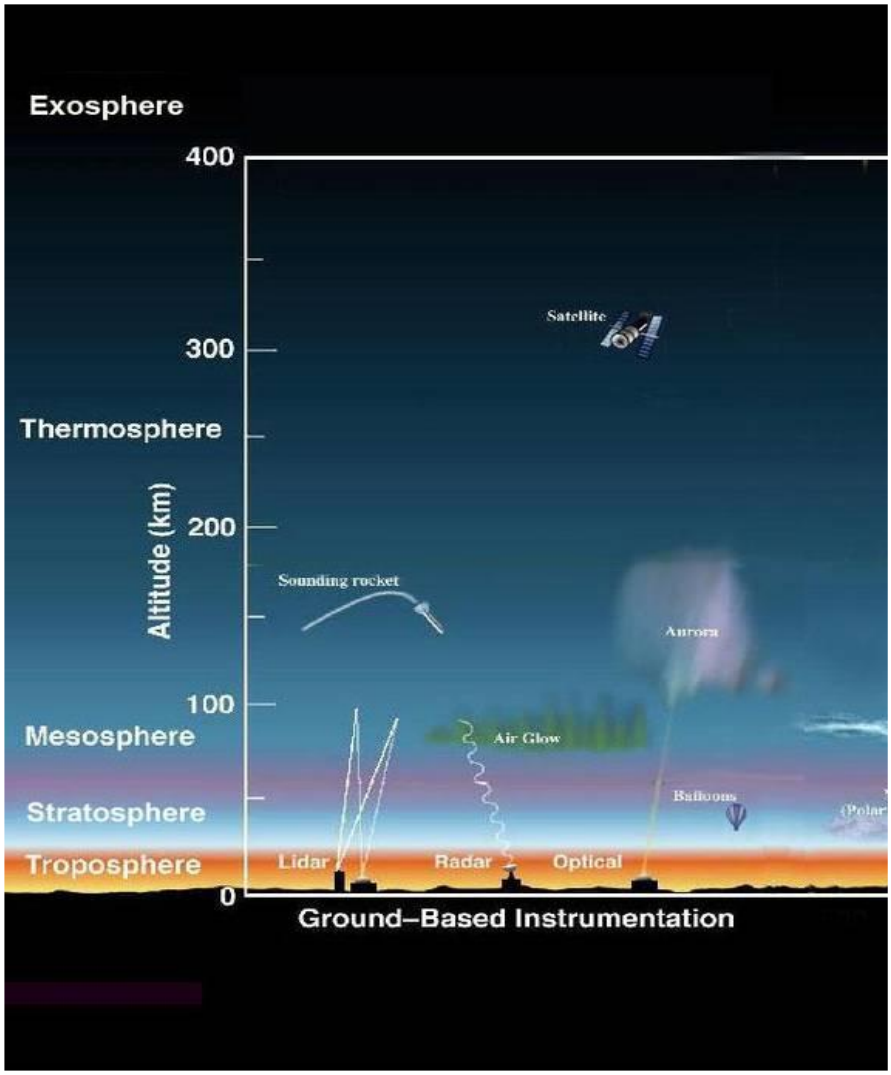

Because of the disparity between these two sets of data, it is obvious that other processes are important to global warming. These processes may occur naturally without human intervention. Figure 2 above strongly suggests that other factors cause increases and decreases in Earth’s atmospheric CO_2 concentrations.

The comparison of these two sets of anomaly data indicates significant uncertainties in the sources of global warming. **Until these uncertainties are resolved, it is unwise to make major political decisions based on current data and models of global warming!**

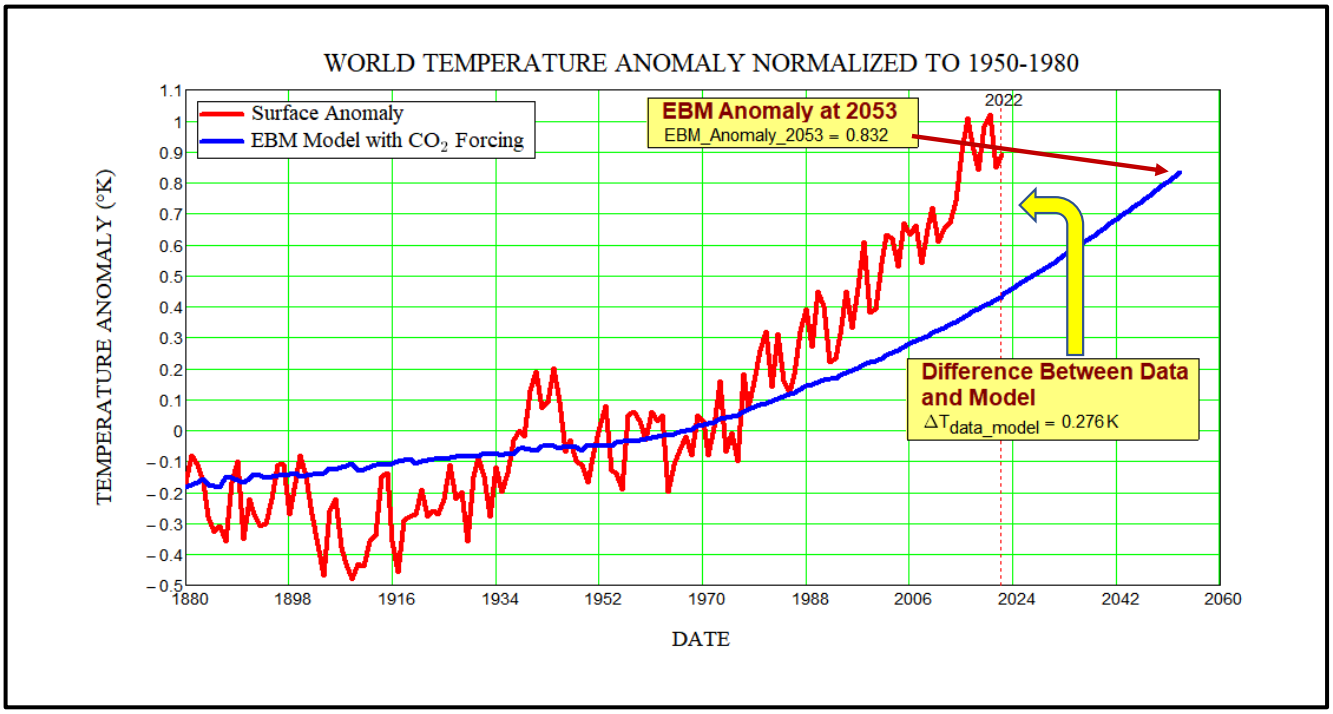

Figure 6. Surface Temperature Anomaly WRT Average Temperature 1950–1980

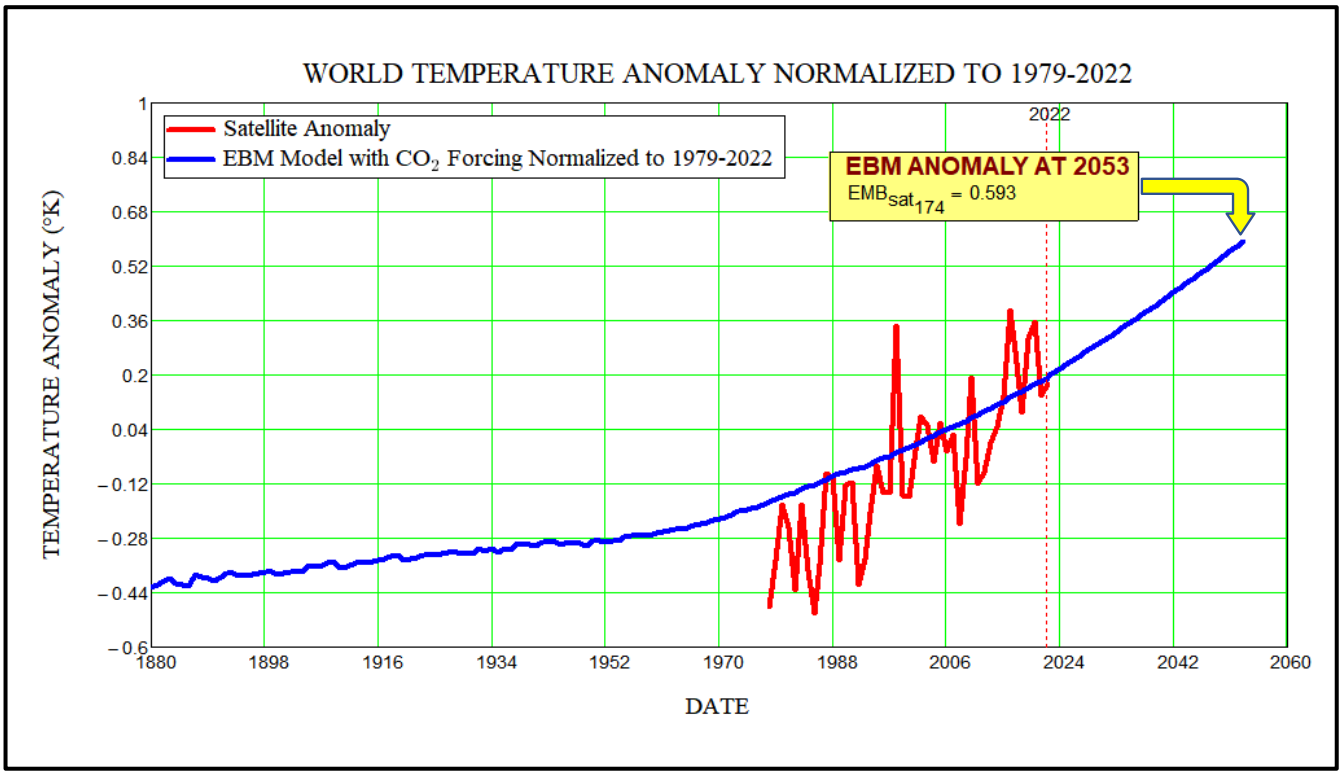

Figure 7. Satellite Temperature Anomaly Normalized to 1979-2022

5. ONE LAYER ATMSPHERE MODEL

5.1. BASIC MODEL

Now we will extend our climate model to a more sophisticated version that includes a single layer atmosphere. The basics of this model are depicted in **Figure 8**.

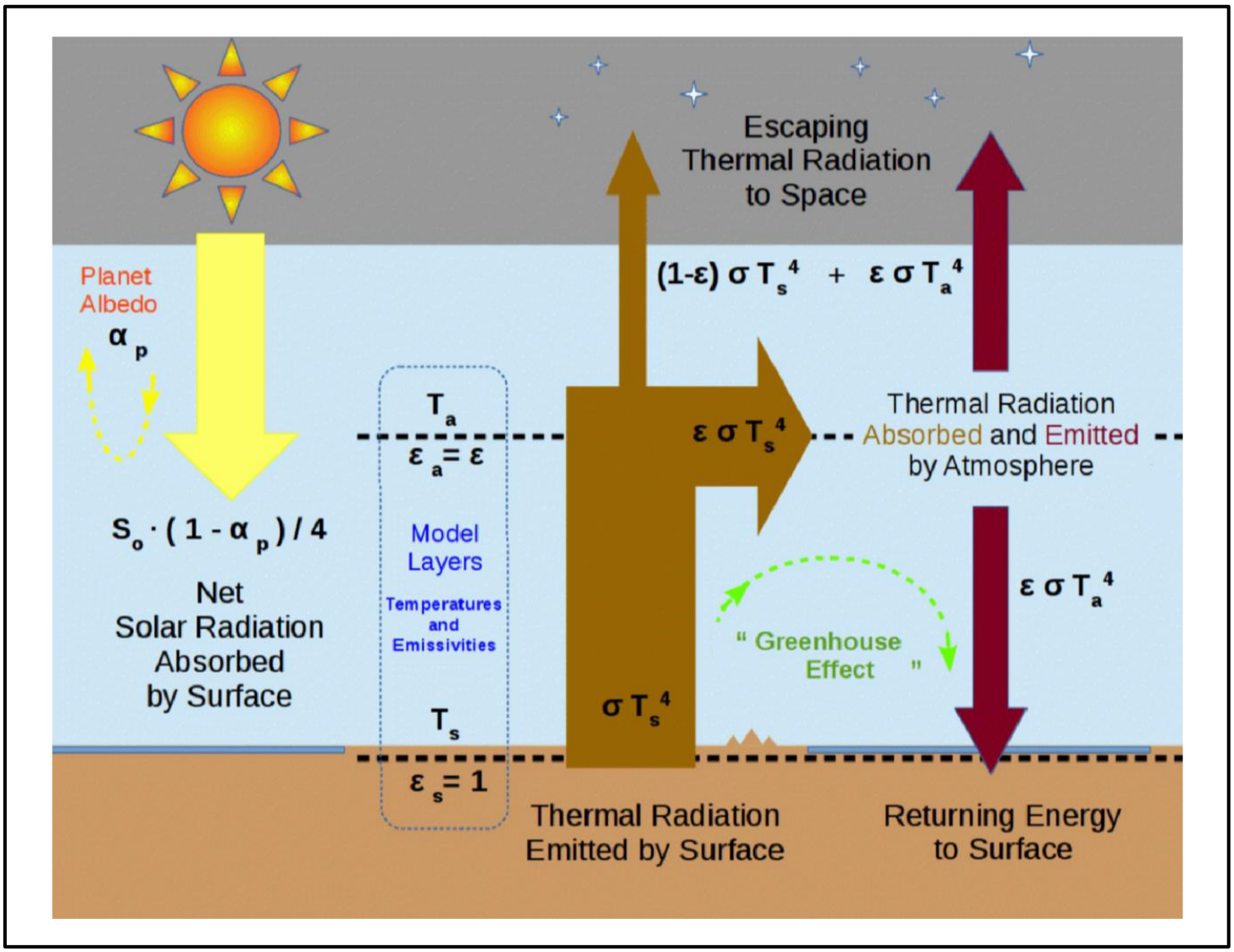

Figure 8. Basics of a Single Layer Atmosphere Model

Referring to **Figure 8**, we have the following energy balance equations. Now, ε = the emissivity and the absorption coefficient of the air.

The energy balance at the top of the atmosphere is:

$$\frac{S_o(1-\alpha_p)}{4} = (1-\epsilon)\sigma T_s^4 + \epsilon\sigma T_a^4 \qquad (6)$$

And at the Earth's surface, the energy balance is:

$$\frac{S_o(1-\alpha_p)}{4} = \sigma T_s^4 - \epsilon\sigma T_a^4 \quad (7)$$

Solving for our new Ts based on this model, we have the following.

$$T_s = \sqrt[4]{\frac{S_o(1-\alpha_p)}{4\sigma\left(1-\frac{\varepsilon}{2}\right)}} \quad (8)$$

The emissivity (or absorption coefficient) of the air versus surface temperature is shown in the following figure, along with a log-log fit to the emissivity [7]. If the emissivity and absorptivity are both zero, no radiation from the surface will be absorbed. This is identical to the energy balance for Earth acting as a black body in the absence of an atmosphere. To obtain our absorption coefficient (ε), we use the surface temperatures from the simple CO_2 EBM.

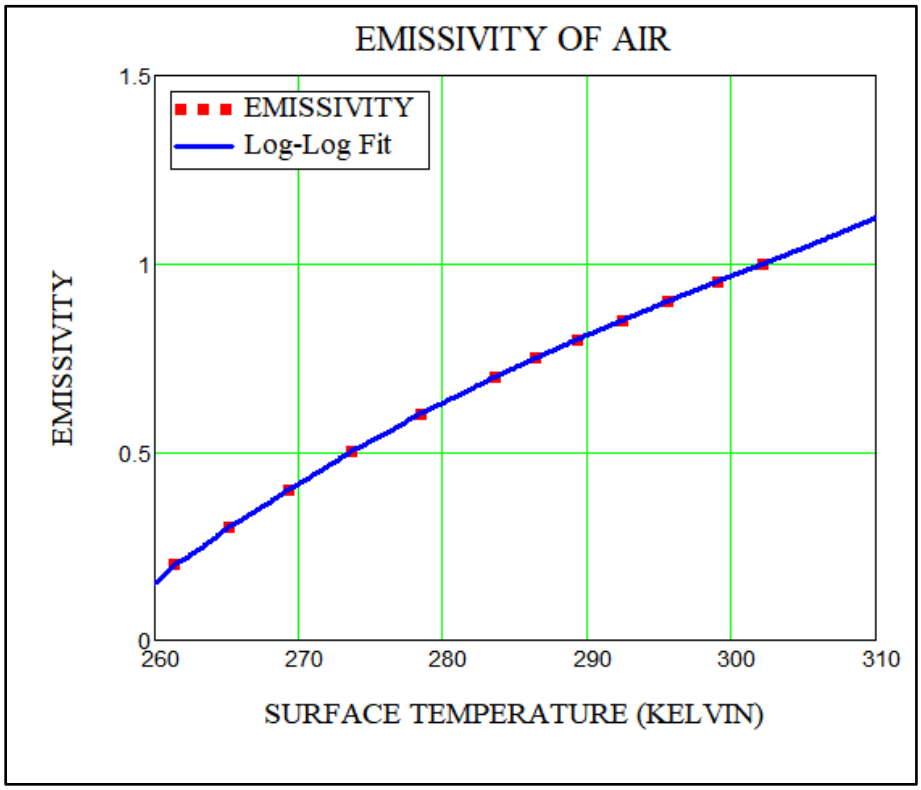

Typical results for the temperature anomalies based on this improved model are shown in **Figure 9**. Note that the one-layer atmosphere model is also normalized to the satellite data normalization between 1979 and 2022. Comparing Figures 7 and 9, we observe that this one-layer atmosphere model is essentially equal to the EBM. This is not very surprising since ε for this model comes from the temperatures of the CO_2 forcing EBM.

Note from Figures 6, 7 and 9 that the models and data depend on the normalization factor. That is why presenting the data as anomalies is confusing since each set is normalized to a different value. Later, we will normalize all data and models to the same date range to reduce the chance of

misinterpretation of the results and the prediction of future global warming. If absolute temperatures were used, this confusion would not occur. Unfortunately, measurement data is only available as anomaly data normalized to a specific date range. Only the surface data provides the normalization factor of T_o= 14 ºC in the date range 1950–1980. This fact will be used later to normalize everything to one factor.

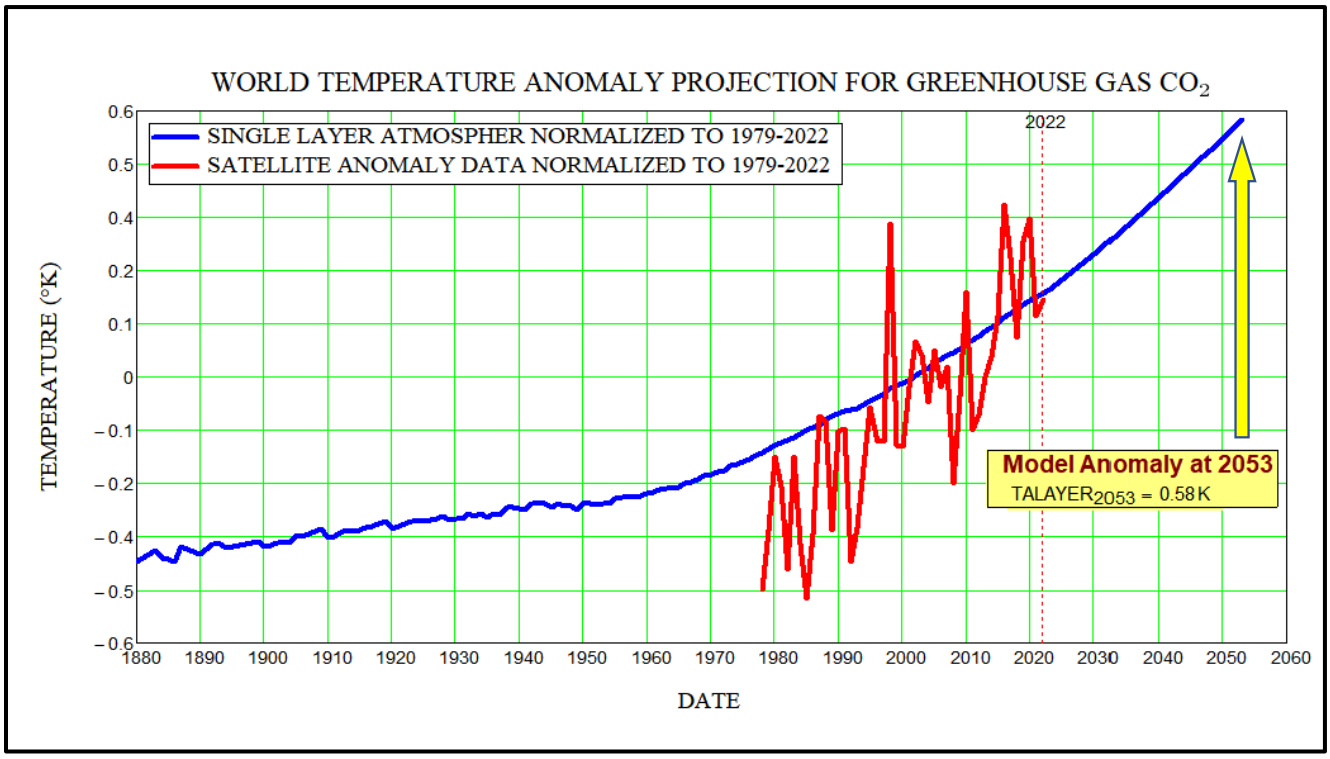

Figure 9. One Layer Atmosphere Model Compared with Satellite Data

Again, there is significant uncertainty in these models and data. Although more sophisticated models might better fit each set of data, the models will be different depending on the measurement data used and the assumptions made in the models. Thus, as before, making major regulations concerning carbon emissions is not well founded at this time.

5.2. DELAY TO EQUILIBRIUM

Recall our First Law of Thermodynamics equation for calculating the Earth's temperature T_s.

$$C\frac{dT_s}{dt} = \frac{S(1-\alpha)}{4} - (\epsilon\sigma T_s^4) \tag{9}$$

Up to this point, we have assumed equilibrium to solve for T_s; however, it takes several years to reach equilibrium. First, we will include CO_2 forcing as described in Section 4. This changes our time dependent thermodynamic equation to the following.

$$C\frac{dT_s}{dt} = \frac{S(1-\alpha)}{4} + \Delta F_{CO_2} - (\epsilon\sigma T_s^4) \tag{10}$$

Now we solve this non-equilibrium equation versus time via finite difference to step time forward in increments of Δt as noted in **Figure 10**. The results demonstrate equilibrium is achieved only after

about 26 years! Therefore, the above analyses, which assume equilibrium, must be amended to include the transient delay to equilibrium.

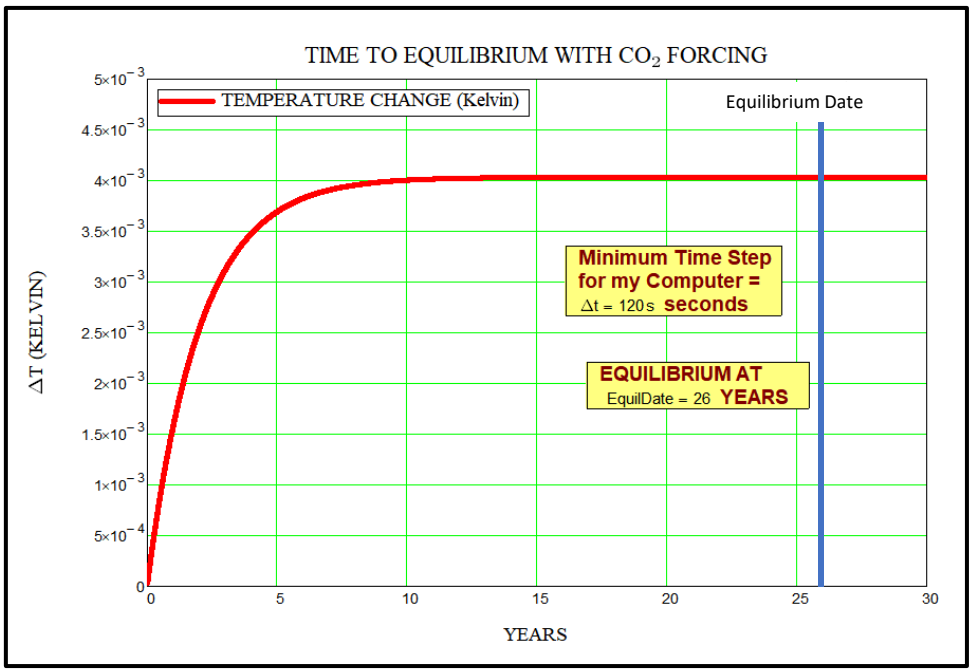

Figure 10. Delay to Reach Equilibrium

We include this delay in our one-layer atmosphere model calculation by delaying the absorption coefficient ε because that is the variable tied to the time-dependent CO_2 forcing function [8]. Including this twenty-six-year delay produces the following climate model results at each equilibrium state in **Figure 11**. These results are in absolute temperature. Normalization is not included.

The delay effect is significant. The magnitude of the difference between models with and without delay is reduced when each model is normalized to one specific time range. Normalization to different time ranges leads to a misinterpretation of the results. Since each set of data is normalized to a different time period, comparisons between different sets of data and models become specious. In Section 7, I have normalized everything to the same time period to compare with the satellite data. I caution again that there are large uncertainties in both models and actual Earth temperature data.

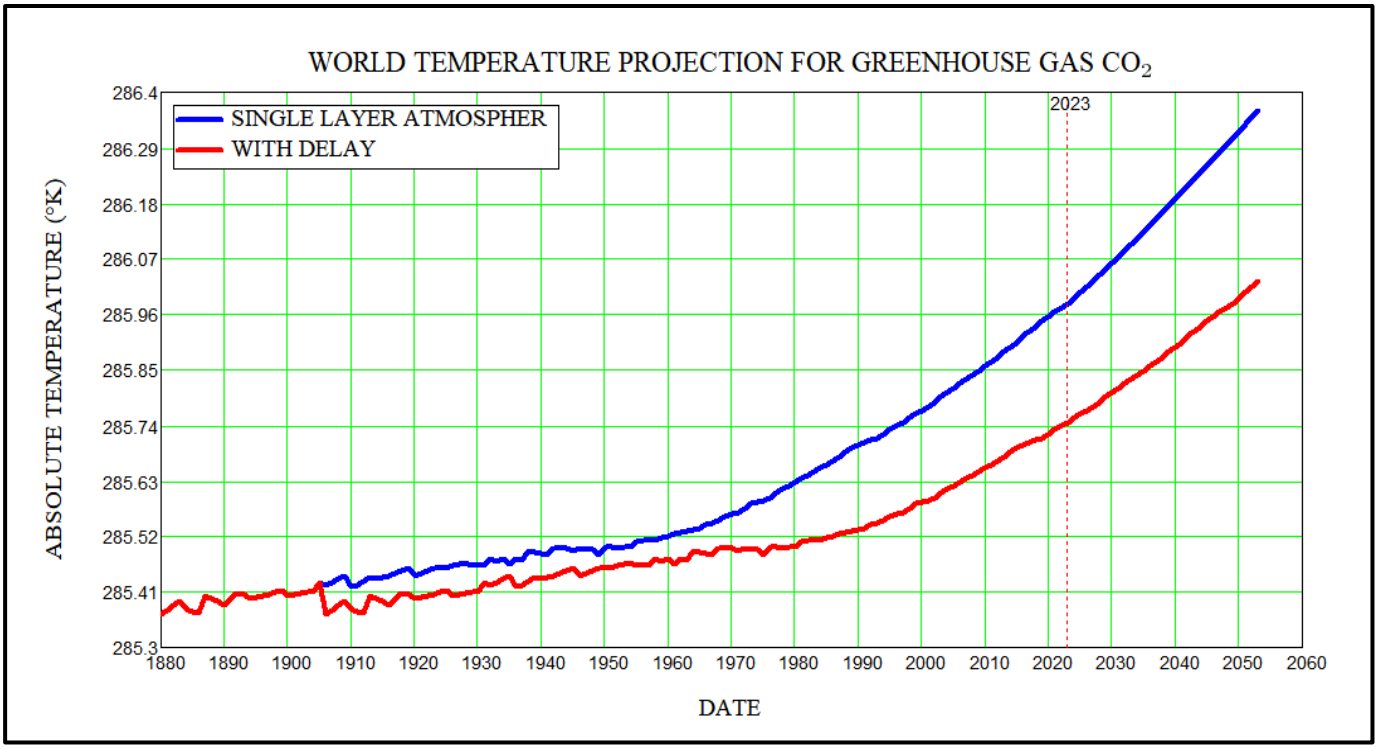

Figure 11. Effect of Delay to Reach Equilibrium on 1-Layer Model

6. EXTRAPOLATIONS TO 2100

6.1. EQULIBRIUM MODEL

It was previously noted that the average of each set of anomaly data is normalized to zero at different time ranges. The surface temperature is normalized between 1950 and 1980. The satellite data is normalized between 1979 and 2022. As noted, this leads to confusing results and misinterpretation of results. Because the surface data has provided its own normalization factor of T_o = 14 °C, this normalization has been removed to produce absolute temperatures. Then, these absolute temperatures are normalized to the satellite data normalization between 1979 and 2022.

Using the satellite and surface data over this normalization date range, each data set is extrapolated to 2100 to compare with the above one-layer atmosphere equilibrium model. The extrapolations are from a least-squares power curve regression. These regressions are of the form $a \cdot x^b + c$, where a, b, and c are chosen to best approximate the data. These results are compared with the one-layer atmosphere equilibrium model, including the delay to equilibrium, in **Figure 13**.

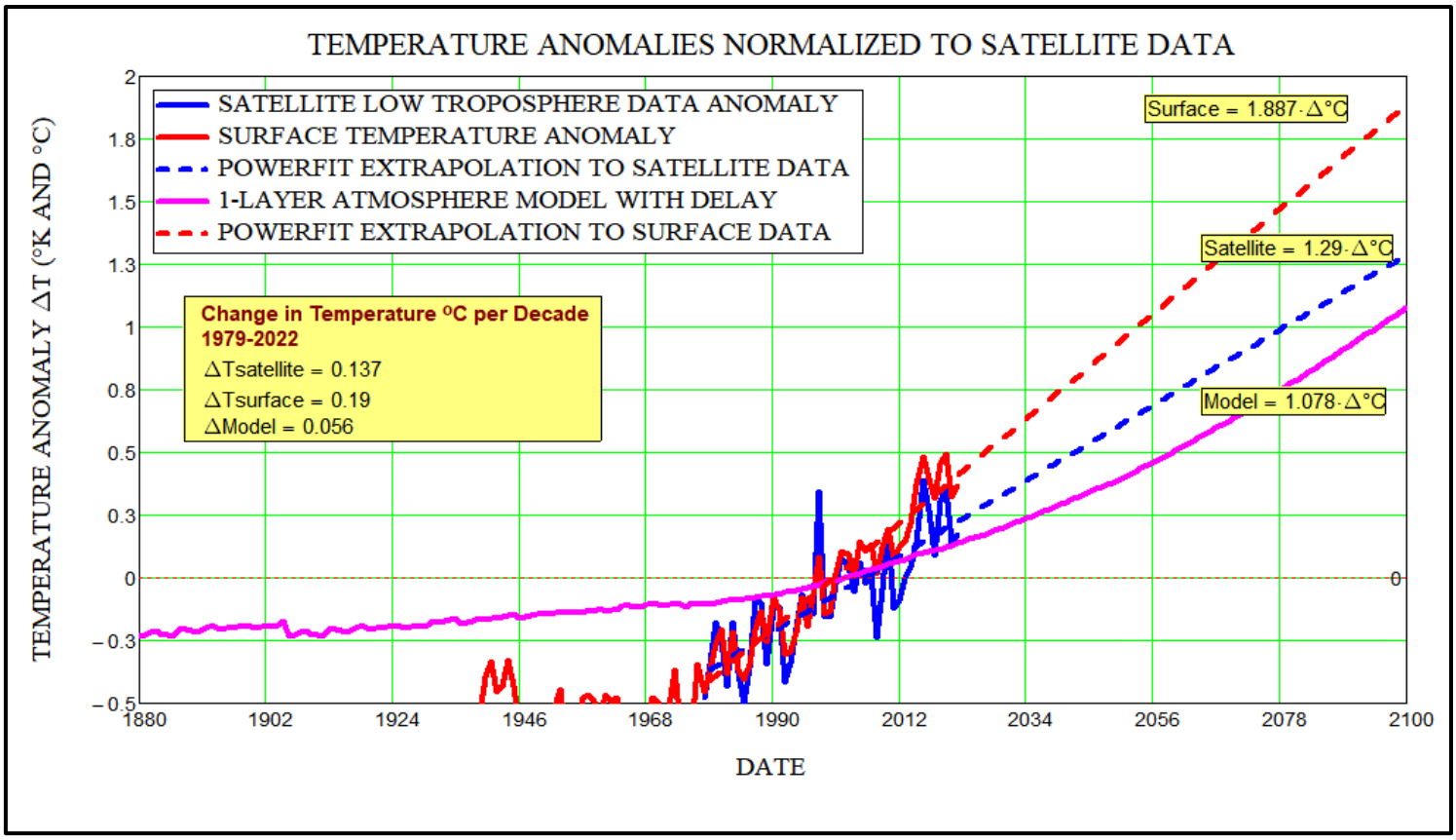

Figure 12. Temperature Anomaly Data Extrapolations vs. 1–Layer Atmosphere Model

The surface temperature anomaly data indicate a more severe warming than either the satellite data or the one-layer equilibrium model with delay. Notice that the extrapolated value for the NASA surface data reaches a temperature anomaly of 1.0 °C in 2053 and a value of 1.9 °C by 2100. However, the satellite data extrapolation, and the one-layer atmosphere equilibrium model are well below this value. Recall, anomalies are differences in temperature; differences in Kelvin and Celsius are equal.

The predicted temperature anomaly in 2053 from the one-layer atmosphere equilibrium model is 0.43 ℃ or ºK. Although not shown, it is similar to the results without delay because each is normalized to match the normalization of the satellite data. This is another reason climate models and data should be reported in absolute temperatures.

The preponderance of evidence indicates that the temperature increases are well within tolerable levels for the next thirty or more years. There is ample time to employ any necessary mitigation in a rational and practical manner. Draconian measures are not warranted by the dominant amount of data or simple models.

6.2. FINITE DIFFERENCE MODEL

One last model is used in our analyses. In addition to the above analyses using energy balance at equilibrium, I have also solved the First Law of Thermodynamics for the Earth's climate using finite difference techniques. Recall our thermodynamic equation.

$$C\frac{dT_s}{dt} = \frac{S(1-\alpha)}{4} + \Delta F_{CO_2} - (\epsilon\sigma T_s^4).$$

Now, recall the linearization of the $\varepsilon\sigma T_s^4$ to give $A + B(T_s - T_o)$. We now write our thermodynamic equation as follows, and we include notation defining which variables are time dependent.

$$C\frac{dT_s(t)}{dt} = \frac{S(1-\alpha)}{4} + \Delta F_{CO_2}(\mathrm{t}) - \big(A + B(T_s(t) - T_o)\big). \qquad (11)$$

The solar energy flux is assumed to be constant because its variation in the past has been so small that it has little effect on the time variation of the surface temperature. This model could be extended to include forcing functions from methane gas, volcano eruption aerosols, and human aerosols; however, those are small perturbations to the CO_2 forcing. Also, the original objective was to determine the effects of CO_2 emissions on global warming.

I ran this model from 1880 to 2100 using two extrapolations for the CO_2 concentration in the atmosphere. In addition to the third-order polynomial, I included an exponential fit and extrapolation in exactly the same manner as the polynomial fit and extrapolation. The extrapolations are presented in **Figure 14**.

The results of this model are compared with the NASA surface data and the satellite data, as we did before in Figure 13. For a fair comparison, everything is normalized to the satellite data as before. The results are shown in **Figure 15**.

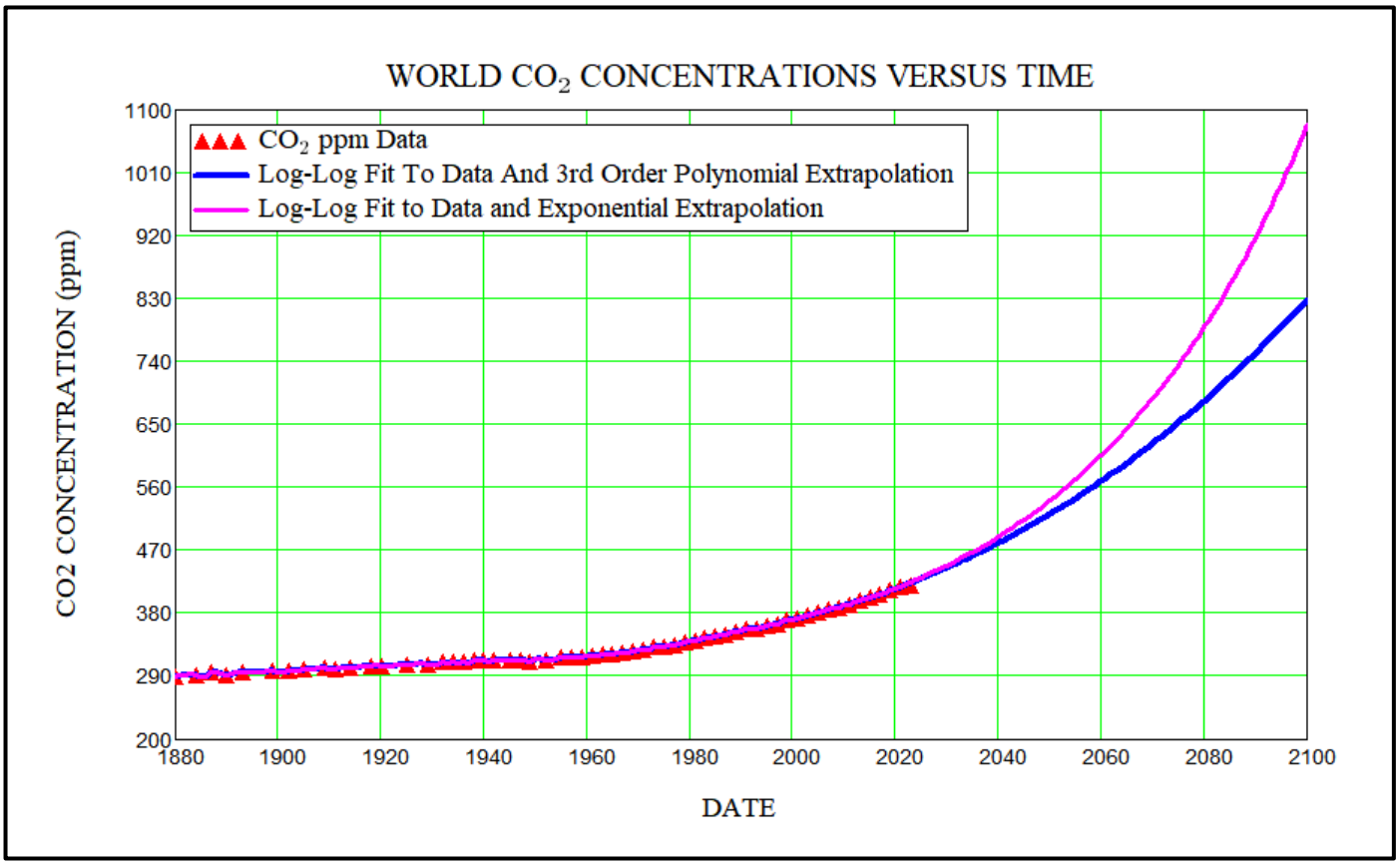

Figure 13. CO_2 Concentration Extrapolations

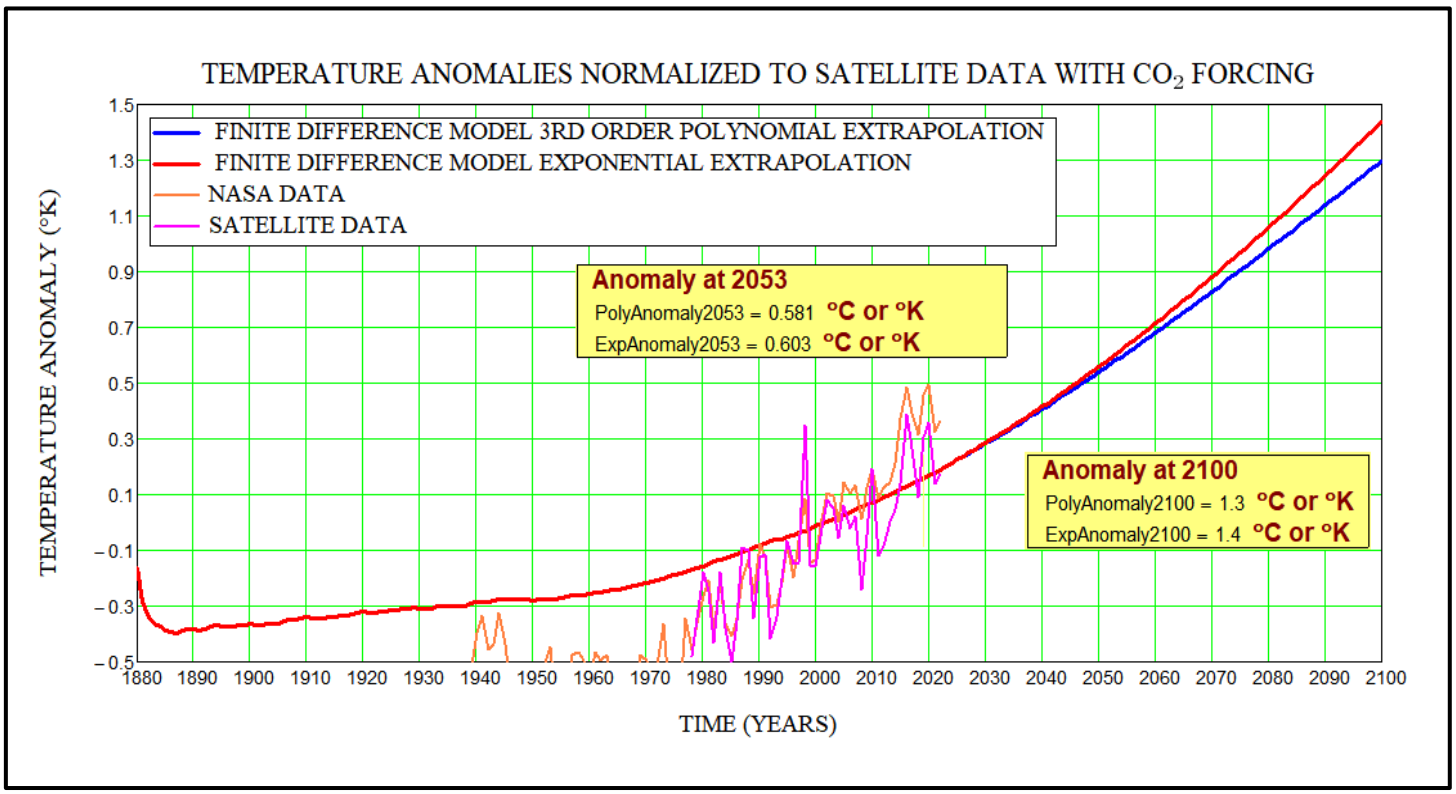

Figure 14. Temperature Anomaly Data Compared with the Finite Difference Solution to the Thermodynamic Differential Equation

Several of the results are worthy of special note.

1. None of the extrapolations come close to the 5 °C anomaly that many climate publications warn about for catastrophic climate effects by 2100.
2. Neither of the finite difference models approaches the NASA surface data extrapolations of Figure 13, even after the NASA data is normalized to the lower satellite data.
3. Both finite difference extrapolations are within 0.1°C of the extrapolated satellite data.

Therefore, this study cannot establish sufficient evidence of catastrophic global warming before 2100. There is clearly sufficient time to mitigate any potential global warming issues without resorting to severe restrictions on the world economy and society in general.

7. ANOMALY STUDY USING YEARLY EMISSION DATA

The analyses in the previous sections used the NASA CO_2 Concentration data to account for the atmospheric contribution to the surface temperature anomalies. Data for yearly emission is also available[11] and has been used by various climate studies to predict severe global warming.

The yearly emission data plus an exponential fit to the data is shown in **Figure 15**.

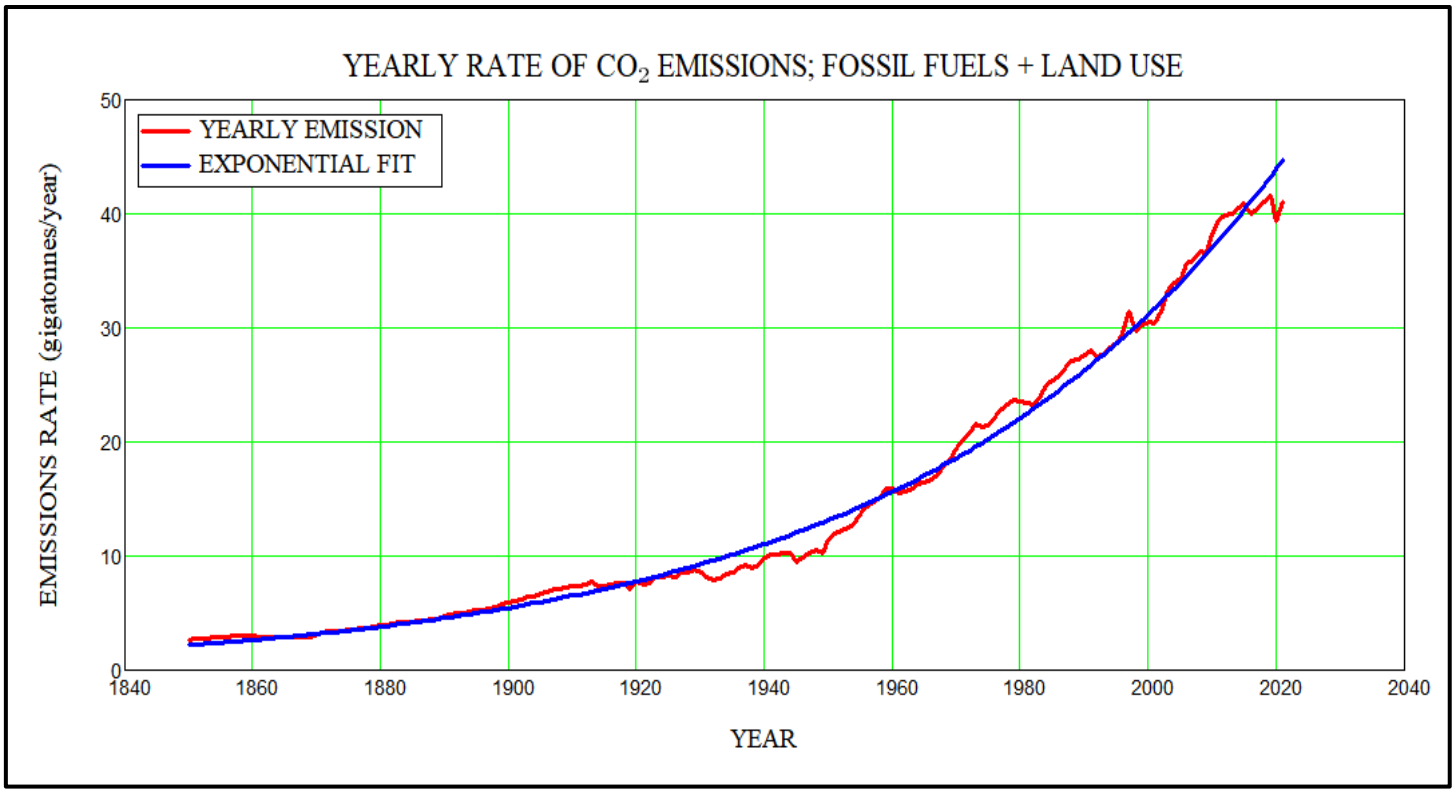

Figure 15. Yearly CO_2 Emissions Including Land Use

The land use noted in the figure title is the contribution to emissions from deforestation since reduction of the biomass causes less CO_2 to be absorbed from the atmosphere. Recall, that plants take up CO_2 and release oxygen in the photosynthesis process.

Calculating the CO_2 emission contribution to global warming is a little more involved than using the CO_2 concentration values. For this, the concentration values are calculated from the emissions minus the sinks of CO_2 in the atmosphere. This is expressed by the following differential equation for the concentration of CO_2 in the atmosphere versus time.

$$\frac{dC(t)}{dt} = Q(t) - \lambda C(t) \tag{12}$$

Where $Q(\mathrm{t})$ is the yearly emission rate from Figure 15. For simplicity, all sinks are lumped into one sink defined by an exponential decay. λ is the decay constant for the exponential decay of the CO_2 concentration in the atmosphere, where $1/\lambda = \tau$, the decay time. τ is assumed to be 500 years for this study because it most closely matches the running sum of the yearly emissions as shown in **Figure 16**. $\mathrm{C(t)}$ is the concentration of CO_2 versus time. The differential equation could be solved by finite difference techniques using the yearly emission data of Figure 15. However, to obtain a closed form solution, an exponential fit to the data, as shown by the blue line of Figure 15, is used for $\mathrm{Q(t)}$. That exponential fit is given by the following.

$$Q(t) = ae^{bt} + c \tag{13}$$

The analytic solution to (12) is given by the following, without proof.

$$C(t) = e^{-\lambda t}\int_0^t e^{\lambda s}Q(s)ds \tag{14}$$

Substituting (13) into (14) and integrating yields the following for the CO_2 concentration versus time.

$$C1(t) = e^{-\lambda t}\left[\frac{a\left[e^{(\lambda+b)t} - 1\right]}{\lambda + b} + c\left[\frac{\left[e^{\lambda t} - 1\right]}{\lambda}\right]\right] \tag{15}$$

Closer examination of the yearly emission data shows that in recent years the emissions have leveled off. From 2014 to the end of the data, the emission is essentially unchanging. The average of the emission data over that time span is 40.362 gigatonnes/year. A linear regression over the same time span varies from 40.57 to 40.67 gigatonnes/year. Therefore, the value from 2014 to 2021 is assumed to be the value at 2021, or 40.67 gigatonnes/year. The solution to the yearly concentration differential equation is given by (15) from t = 0 to t_o = 2021. Fixing $\mathrm{Q(t)}$ to a constant value of C_o = 40.67 gigatonnes/year for $t \geq t_o$ gives the following result.

$$C(t) = \frac{-C_0\left[e^{\lambda(t_o - t)} - 1\right]}{\lambda} + C1(t_o);\ \ t \geq t_o \tag{16}$$

Using (15) and (16) over the total time range gives the following results shown in **Figure 16,** after gigatonnes are converted to parts per million (ppm). A gigatonne is a metric tonne, or 1,000 kilograms.

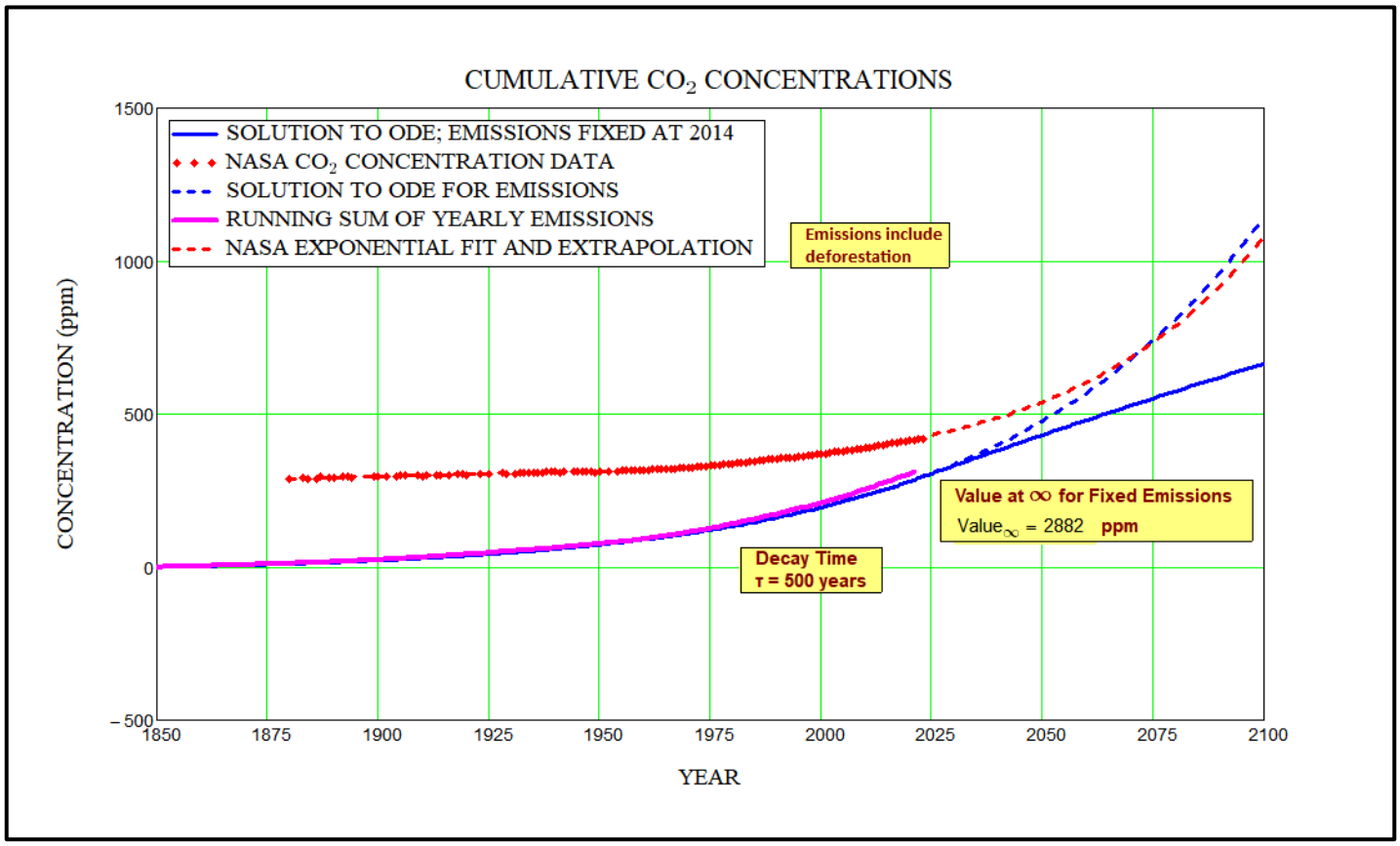

Figure 16. CO_2 Concentrations from NASA Data and Yearly Emissions

Although past and present CO_2 concentrations from the yearly emissions method are significantly lower than the NASA concentrations, future projections are similar for the case where the yearly emissions are not fixed at 2021 and beyond.

Using the concentrations of Figure 16 and Figure 13 to compute CO_2 forcing, anomalies for global warming are provided in **Figure 17**.

The anomaly using the NASA concentration data plus the exponential extrapolation has not been normalized to the satellite data as was done in Figure 14. The results from the emissions data without fixing emissions at 2021 is 2.3 ^oC at 2100 compared with 1.6 ^oC for the NASA CO_2 concentration data forcing, including the exponential extrapolation.

Notice that fixing the emissions at the 2021 value produces a curve that approaches the NASA concentration curve. The emissions-fixed curve is approaching a finite asymptotic value. Review of equation (16) indicates that this asymptotic value at t = ∞ is equal to:

$$C(t \to \infty) = \frac{-C_o\left[e^{\lambda(t_o - t)} - 1\right]}{\lambda} + C1(t_o);\ \ t \to \infty \tag{17}$$

This asymptotic value is $C(t{=}\infty)$ = 22,566 gigatonnes, which transforms to 2882 ppm. This leads to an asymptotic value for the temperature anomaly of 3.7 ^oC (not shown).

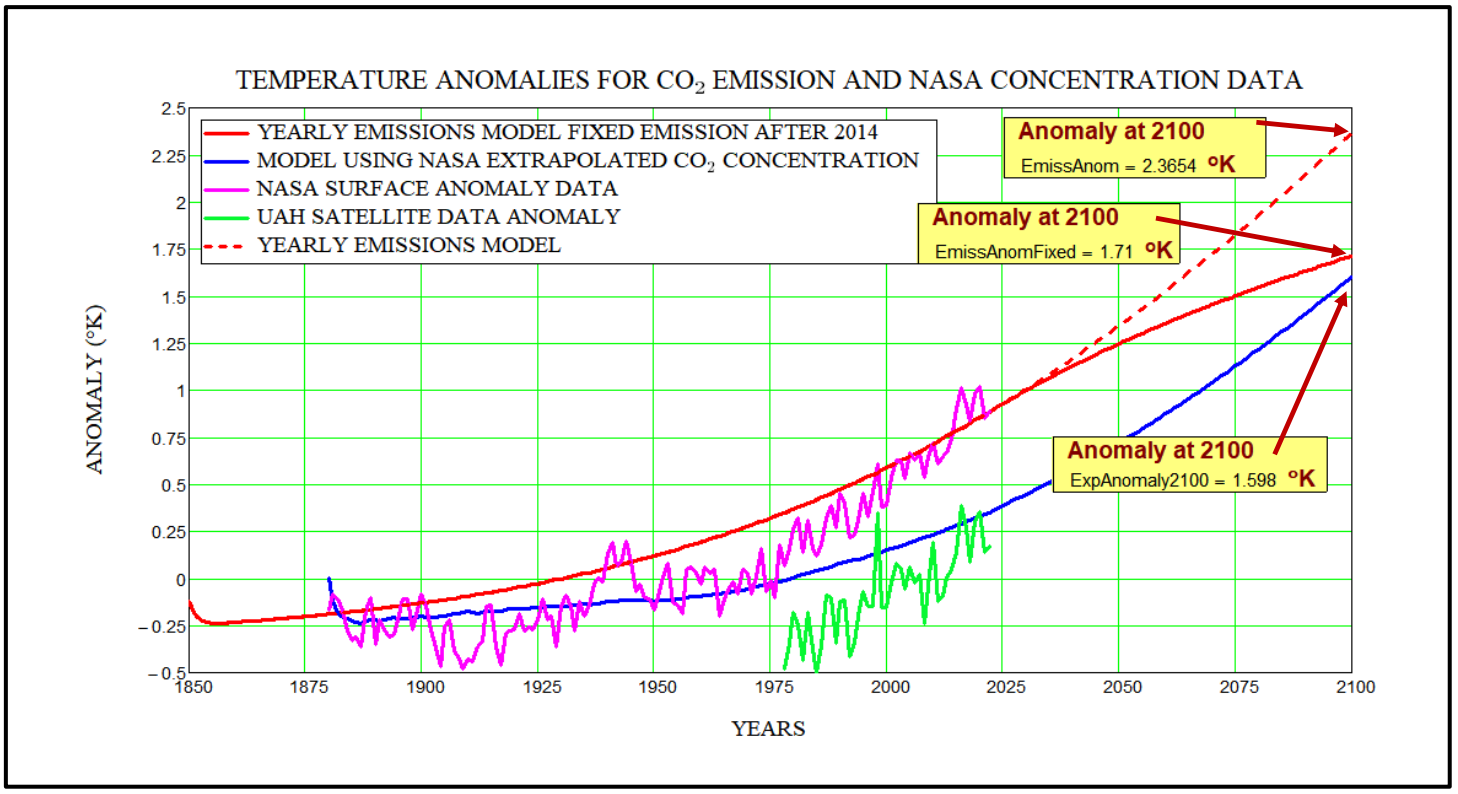

Figure 17. Temperature Anomalies for Emissions and Concentration Data

Although the 1.5 ℃ is exceeded by 2100, the CO_2 emission model does not predict catastrophic warming if the recent constant value of emissions is included in the model.

8. ALBEDO SENSITIVITY STUDY AND NOAA-STAR SATELLITE DATA

The above satellite data from Reference [6] is generally referred to as the University of Alabama, Huntsville (UAH) satellite data. NOAA has recently published an independent set of their satellite data, referred to as the NOAA-STAR satellite data. Zou et.al. have analyzed the most recent data (STAR V5.0) and provided summary results in Figure 14 of their report[10]. **Figure 18** compares the NOAA-STAR data with the UAH data. Both sets of data have been converted to yearly averages.

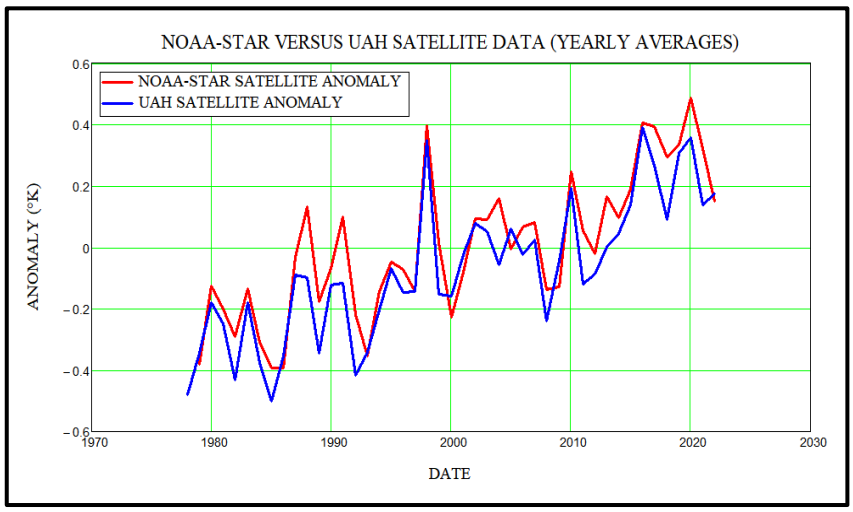

Figure 18. Comparison of NOAA-STAR with UAH Satellite Data

Because the data sets are so similar, the albedo sensitivity study is compared with the UAH data in the following discussion.

To determine how sensitive the models are to small variations in the Earth's albedo, I ran the finite difference model of Equation (11) for $\alpha = 0.317$ to 0.322, a spread of only 1.6% in the albedo

value. The value for the albedo used to this point in the study was 0.32, a common published value. The results of this sensitivity study are presented in **Figure 19**.

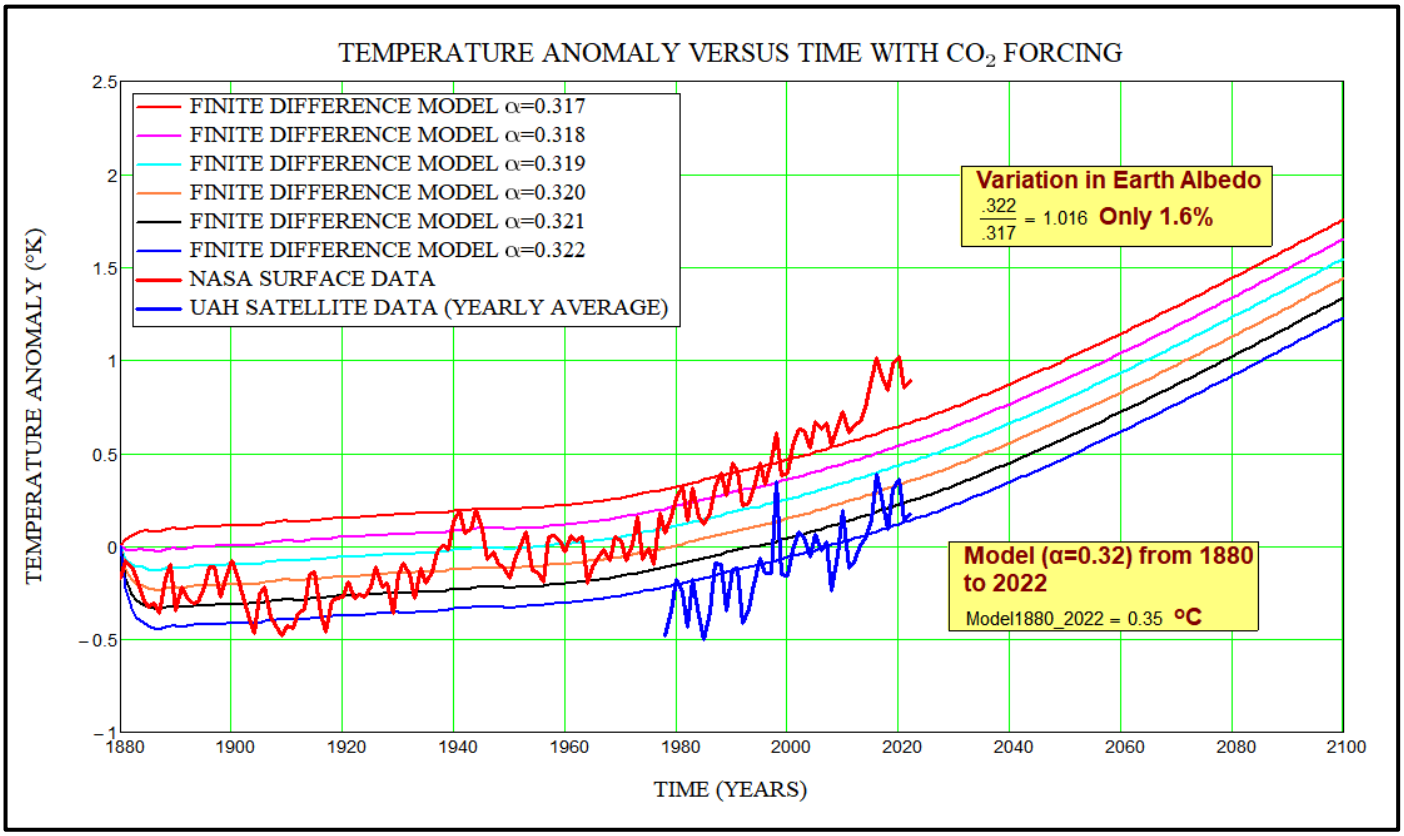

Figure 19. Model Sensitivity to Albedo Variations

It is clear that extremely small variations in the Earth's average albedo have a very large effect on the model temperature anomalies.

Such sensitivities in models make the whole process specious. It is just as accurate to fit the existing warming data with a regression technique and use that to predict future values. Then we are left with which set of data to believe: surface or satellite data. This disparity in data makes the prediction of warming suspect. It is clear that there is global warming and a simultaneous increase in CO_2. The question is how much global warming will occur in the future and how much is anthropogenic. An open question is whether or not CO_2 is the main cause of the warming; water vapor is a more forcing greenhouse gas. The global warming question is not 100% settled and the debate is not over.

9. RECENT DATA INDICATING LITTLE GLOBAL WARMING

9.1. STABILITY OF SATELLITE DATA OVER MORE THAN EIGHT MONTHS

For more than eight years, the satellite data has shown essentially no global warming. This is demonstrated for both the UAH and the STAR satellite data in **Figure 20**. In addition to the actual data, a linear regression fit to each data set is shown. From the regression fit, the UAH data indicates zero change in global warming over the entire range depicted. The STAR data indicates an increase of only 0.02 °C. Both of these represent essentially no change.

These data indicate the fallacy of starting global warming analyses at the beginning of the industrial revolution. One might ask, "Why not start the data analyses at the warm period of the Holocene Temperature Conundrum[9], when the global temperature was warmer than the present day and there were no anthropogenic CO_2 emissions?"

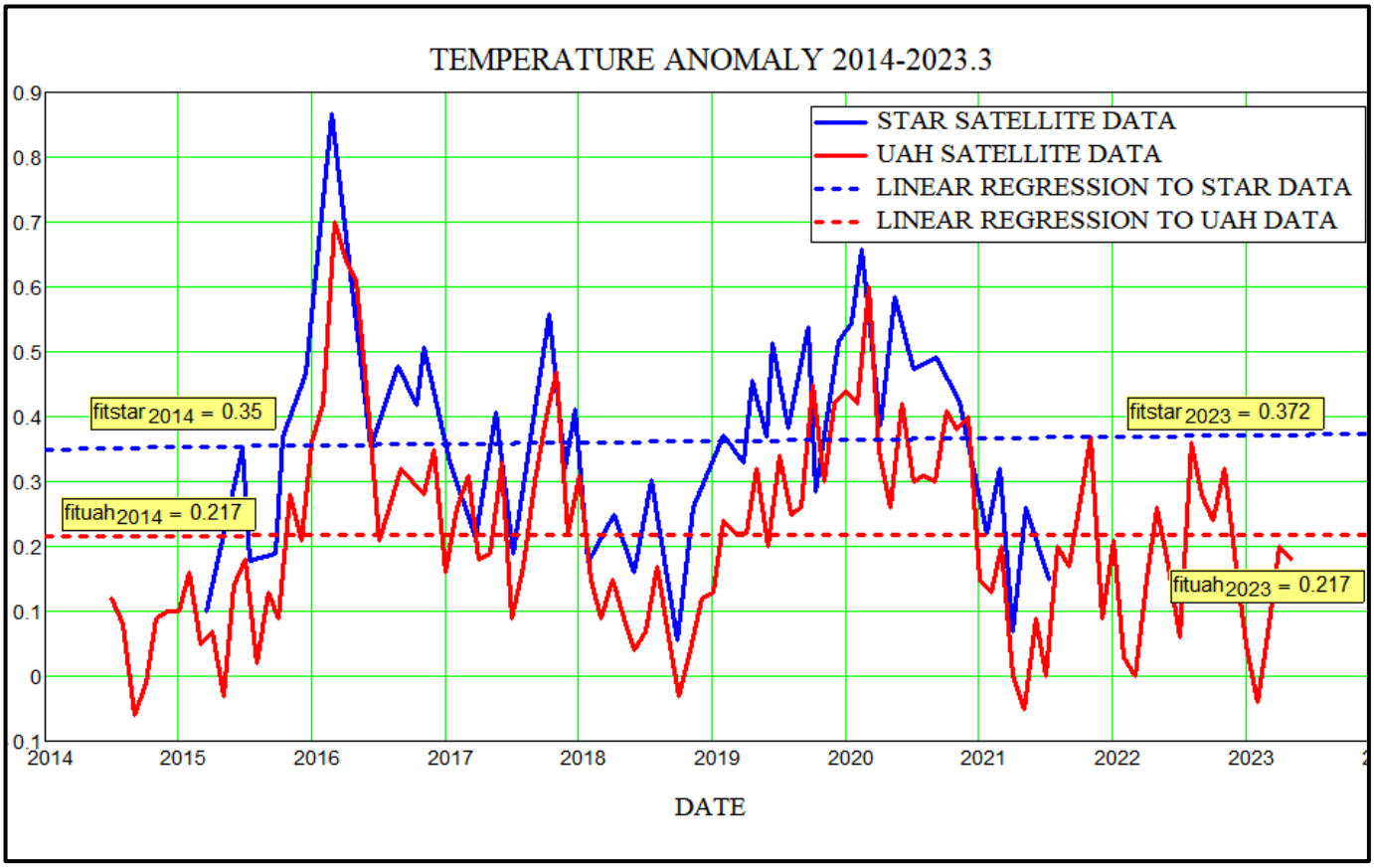

Figure 20. Satellite Temperature Anomalies for 9 Years and 3 Months

In the following section, the above linear regressions are extended to 2100. In addition, the NASA surface anomaly data is clipped to the same reduced time period of 2014 to 2023 for comparison and to remove the beginning of the industrial revolution.

9.2. EXTRAPOLATED REGRESSION FIT TO RECENT DATA

As noted previously, models, especially those based on matching data at the beginning of the industrial revolution, lead to unrealistic catastrophic predictions of global warming. Recent warming data and recent CO_2 emission and concentration data indicate a reduction in the rate of increase. Using the recent anomaly data from all sources, there has been very little temperature increase over the past eight to nine years. This is demonstrated in **Figure 21** for the data sets beginning in 2014. Note that these data sets are detailed data and not yearly averages.

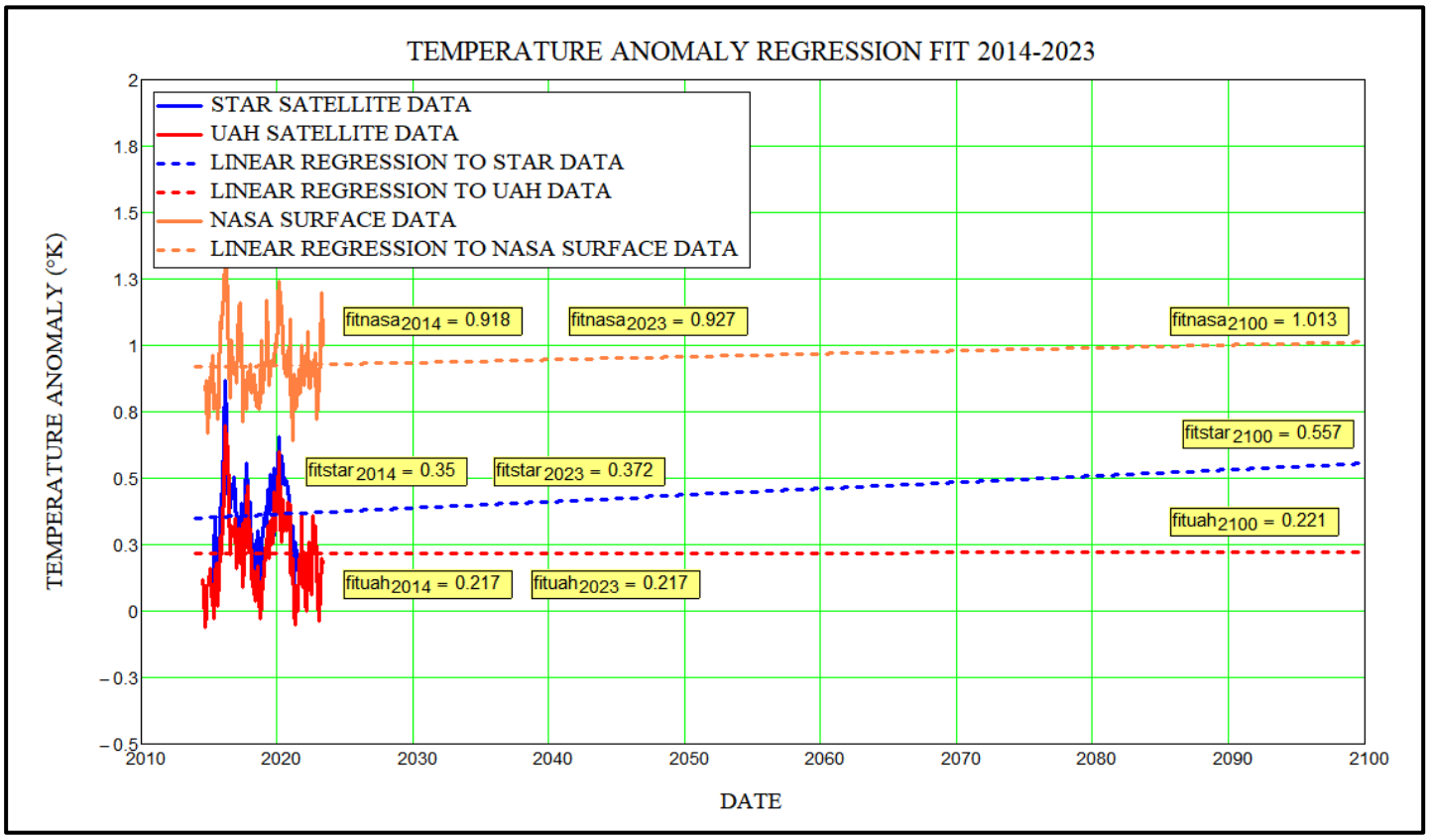

Figure 21. Regression Analysis of Recent Anomaly Data

It is clear that recent anomaly data from all sources indicate very little temperature increase. If the CO_2 emissions and the temperature anomalies remain stable, there is little cause for concern about global warming, at least through 2100.

10. CONCLUSIONS

The primary conclusions from these data and analyses are as follows:

1. Greenhouse gases are critical to warming the Earth to habitable levels for human existence. Otherwise, the Earth would be a frozen planet.

2. This report has presented numerous models and compared those models with actual data. It is clear that these models are sensitive to various assumptions and parameter values, such as the average global albedo and the start time of the analyses; therefore, they predict unrealistic levels of global warming.

3. Extrapolation of the data is as good, if not better than models, at predicting future global warming.

4. Because recent data exhibits very little surface warming, comparisons of recent data and models to the beginning of the industrial revolution predict unrealistic levels of future global warming. One might ask, “Why not start the data analyses at the warm period of the Holocene Temperature Conundrum, when the global temperature was warmer than the present day in

the absence of anthropogenic CO_2 emissions?" See Reference [9].

5. Two totally independent measurements of surface temperature exist: surface measurements and satellite measurements. They are significantly different and predict significantly different values for future global warming.

6. More sophisticated models than those included herein might fit at least one set of data better; however, they will not fit all sets until the disparity between the data sets is resolved and included in the models.

7. Clearly, there is global warming and an increase in CO_2. It is much less clear how much global warming will occur in the future. It is also less clear how much of the warming is due to CO_2 and how much is of anthropogenic origin.

8. **The large disparity between the NASA surface measurements and other data (namely the UAH satellite data and the NOAA-STAR satellite data) must be resolved before giving high confidence to climate change predictions!**

9. **Recent plans to drastically curb fossil fuels are not well supported by the data or models. The resulting radical regulations have potentially catastrophic effects on the world economy and modern society; they should be delayed until the science becomes less uncertain.**

10. **It is clear that the science is not settled, nor is the debate over!**

11. REFERENCES

[1] Dr. Curry holds a Ph.D. in nuclear physics from The University of Texas at Austin. He worked for over 35 years in applied nuclear physics performing research in Nuclear Weapons Electromagnetic Pulse (EMP) phenomena, microwave radiation phenomena and safety, and radiation therapy medical physics to plan radiation treatments for cancer patients. His work in radiation therapy was conducted at the University of New Mexico Cancer Research and Treatment Center and at The University of Texas Medical Branch. His EMP research was conducted at Sandia National Laboratories, Kaman Sciences Corporation, and Mission Research Corporation where he served as a senior scientist and group leader. He was the principal scientist and director of large government contracts with The Defense Nuclear Agency, The Office of Naval Research, and The Department of The Army. All of these EMP efforts involved developing large computer models of the applicable nonlinear physics.

[2] https://www.e-education.psu.edu/meteo469/node/112

[3] https://www.theguardian.com/science/2021/jul/05/sixty-years-of-climate-change-warnings-the-signs-that-were-missed-and-ignored

[4] https://go.owu.edu/~chjackso/Climate/papers/Myhre_1998_New%20eatimates%20of%20radiative%20forcing%20due%20to%20well%20mixed%20greenhouse%20gasses.pdf

[5] https://climate.nasa.gov/vital-signs/global-temperature/

[6] https://www.drroyspencer.com/latest-global-temperatures/

[7] https://www.acs.org/climatescience/atmosphericwarming/singlelayermodel.html

[8] Both the Earth's albedo α and the Solar Constant S are also time-varying. Varying the Solar Constant values over accepted and measured values has little effect on the final results of the anomaly models. Therefore, time-varying S has not been included in this study. On the other hand, small variations in the albedo causes large changes in the anomaly models. This leads to large uncertainty in the model results and predictions of global warming.

[9] https://www.pnas.org/doi/10.1073/pnas.1407229111

[10] https://agupubs.onlinelibrary.wiley.com/doi/10.1029/2022JD037472

[11] https://ourworldindata.org/co2-emissions